Supporting information for

An Isolable Iron(II) Bis(supersilyl) Complex as an Effective Catalyst for Reduction Reactions

Shogo Arata [b] *and Yusuke Sunada** [a,b]

[a]*Institute of Industrial Science, and* [b]*Department of Applied Chemistry, School of Engineering Science, The University of Tokyo, 4-6-1 Komaba, Meguro-ku, Tokyo 153-8505, Japan.*

Contents

General. Manipulation of air and moisture sensitive compounds was carried out under a dry nitrogen atmosphere using Schlenk tube techniques associated with a high-vacuum line or in the glove box which was filled with dry nitrogen. All solvents were distilled purchased from Kanto Chemical Co. Inc., and was dried over activated molecular sieves. ^{1}H and ^{13}C NMR spectra were recorded on a JEOL Lambda 400 spectrometer at ambient temperature. ^{1}H and ^{13}C NMR chemical shifts (δ values) were given in ppm relative to the solvent signals. Elemental analyses were performed by a Thermo Scientific FLASH 2000 Organic Elemental Analyzer. IR spectra were recorded on a PerkinElmer Spectrum Two spectrometer. GC/GC−MS analyses were acquired on a Shimadzu QP5000. Potassium tris(trimethylsilyl)silanide was synthesized by the method reported in the literature.[1] All reagents were purchased from Tokyo Chemical Industries Co., Ltd. or Sigma-Aldrich, and were used without further purification.

Synthesis of $(THF)_2Fe[Si(SiMe_3)_3]_2$ (1). In a 50 mL schlenk tube, $FeBr_2$ (1 g, 4.64 mmol) was suspended in THF (20 mL), then potassium tris(trimethylsilyl)silanide (3.90 g, 9.74 mmol, $K[Si(SiMe_3)_3]\cdot 1.58THF$ in 15 mL THF) was slowly added to this solution at room temperature. The solution was stirred at room temperature for 1 h. The pale brown suspension turned to dark red-purple solution, then the solution was centrifuged to remove the insoluble materials. The mother liquid was evaporated *in vacuo*, and the obtained solid was dissolved in pentane (80 mL). The solution was again centrifuged to remove the insoluble materials. The supernatant was collected, and THF (5 mL) was added. The solvent was concentrated to ca. 15 mL, and the remaining solution was cooled at -30 °C. Complex **1** was obtained as red-purple crystals in 89% yield (2.87 g). ^{1}H NMR (400 MHz, r.t., C_6D_6): δ = 7.27 (brs, 54H, $SiMe_3$), 20.60 (brs, 8H, THF), 27.33 (brs, 8H, THF). Magnetic susceptibility (Evans): μ_{eff} = 5.36 (in C_6D_6, 21 °C). Anal. Calcd. for $C_{26}H_{70}O_2Si_8Fe_1$: C, 44.91; H, 10.15. Found: C, 45.11; H, 10.31.

Synthesis of $(Pyridine)_2Fe[Si(SiMe_3)_3]_2$ (2). In a 50 mL schlenk tube, complex **1** (200 mg, 0.288 mmol) was dissolved in THF (10 mL), then pyridine (46.3 μL, 0.575 mmol) was added to this solution at room temperature. The solution was stirred at room temperature for 1 h. The color of the solution turned from dark red to dark brown. The mother liquid was evaporated *in vacuo*, and the obtained solid was dissolved in pentane (50 mL). The solution was centrifuged to remove the trace amount of insoluble materials. The supernatant was collected, and the solvent was concentrated to ca. 15 mL. The remaining solution was cooled at -30 °C, then **2** was obtained as dark brown crystals in 40% yield (82 mg). Dark brown crystals suitable for X-ray diffraction analysis were obtained by recrystallization from heptane. ^{1}H NMR (600 MHz, r.t., C_6D_6): δ = −13.02 (brs, 4H, pyridine), 6.56 (brs, 54H, $SiMe_3$), 8.36 (brs, 2H, pyridine), 46.69 (brs, 4H, pyridine), Anal. Calcd. for $C_{28}H_{64}N_2Si_8Fe_1$: C, 47.41; H, 9.09; N, 3.95. Found: C, 47.07; H, 9.25; N, 3.56.

Reaction of 1 with pyridine in C_6D_6. In a 20 mL frask, complex **1** (30 mg, 0.043 mmol) was dissolved in C_6D_6 (2 mL), then pyridine (7.3 μL, 0.090 mmol) was added to this solution at room temperature. The solution was stirred at room temperature for 1 h, and quantitative formation of **2** was confirmed by ^{1}H NMR spectrum.

General Procedure for the reduction of carbonyl compounds catalyzed by 1. Catalyst **1** (3.5 mg, 0.005 mmol, 0.5 mol%) was placed in a 10 mL flask, then substrate (1 mmol) and Ph_2SiH_2 (405 mg, 2.2 mmol) were added. The resulting mixture was stirred at r.t. for the time indicated in Table 1 in the manuscript, then complete consumption of the substrate was confirmed by ^1H NMR spectrum. After removal of the volatiles, 6.6 mL of $^nBu_4F$ solution (1M in THF) was added at 0 ^oC, then the mixture was stirred for 3h at r.t. The solvents were removed under reduced pressure, and the residue was dissolved in AcOEt. The solution was washed three times with distilled water (totally 60 mL), and the combined organic layers were dried with brine and Na_2SO_4 (*ca*. 3 g). After removal of the solvent, purification of the residue by silica gel column chromatography (AcOEt/Hexane = 1/4) gave the product.

Spectral data of the products

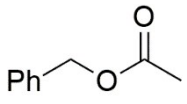

The product was obtained as benzyl acetate after acetylation. The crude prodfuct obtained from the hydrosilylation reaction was treated with $^nBu_4F$, then standard workup shown above was followed. The obtained crude product was treated with acetyl chloride (77.8 μL, 1.1 mmol) and NEt_3 (152.5 μL, 1.1 mmol) in THF (5 mL), then the mixture was stirred overnight at room temperature. The solvenet was removed *in vacuo*, then the prodcut was extracted with diethyl ether (10 mL x 2). The product was purified by silica gel column chromatography (AcOEt/Hexane = 1/4). Isolated yield: 106.4 mg (0.71 mmol, 71%). ^1H NMR (400MHz, r.t. $CDCl_3$) δ: 2.11 (s, 3H, CH_3), 5.11 (s, 2H, CH_2), 7.30-7.39 (m, 5H, C_6H_5). ^{13}C NMR (100MHz, r.t., $CDCl_3$) δ: 21.2 (CH_3), 66.5 (CH_2), 128.4 (C_6H_5), 128.7 (C_6H_5), 136.1 (C_6H_5), 171.0 (CO). IR (ATR): 3091, 3068, 3035, 2958, 2892, 1956, 1738, 1608, 1587, 1498, 1456, 1431, 1380, 1363, 1226, 1082, 1027, 1003, 965, 922, 902, 837, 750, 739, 698, 642, 613, 578, 502.

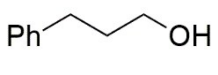

Isolated yield: 117.1 mg (0.86 mmol, 86%). ^1H NMR (400MHz, r.t., $CDCl_3$) δ: 1.42 (brs, 1H, OH), 1.90 (m, 2H, CH_2), 2.72 (t, 2H, J = 8.2 Hz, CH_2), 3.68 (t, 2H, J = 6.4 Hz, CH_2), 7.17-7.22 (m, 2H, C_6H_5), 7.27-7.32 (m, 3H, C_6H_5). ^{13}C NMR (100MHz, r.t., $CDCl_3$) δ: 32.2 (CH_3), 34.4 (CH_2), 62.5 (CH), 126.0 (C_6H_5), 128.55 (C_6H_5), 128.57 (C_6H_5), 142.0 (C_6H_5). IR (ATR): 3332, 3087, 3063, 3027, 3003, 2940, 2864, 1950, 1880, 1807, 1744, 1603, 1583, 1496, 1472, 1454, 1154, 1058, 1031, 918, 810, 745, 699, 574, 521, 495.

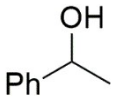

Isolated yield: 106.1 mg (0.87 mmol, 87%). ^1H NMR (400MHz, r.t., $CDCl_3$) δ: 1.50 (d, 3H, J = 6.4 Hz, CH_3), 1.64 (brs, 1H, OH, overlapped with water), 4.91 (q, 1H, J = 6.4 Hz, CH), 7.27-7.40 (m, 5H, C_6H_5). ^{13}C NMR (100MHz, r.t., $CDCl_3$) δ: 25.3 (CH_3), 70.6 (CH), 125.5 (C_6H_5), 127.7 (C_6H_5), 128.7 (C_6H_5), 145.9 (C_6H_5). IR (ATR): 3352, 3084, 3064, 3029, 2973, 2928, 2874, 1602, 1493, 1451, 1429, 1368, 1305, 1285, 1203, 1100, 1077, 1029, 1010, 997, 898, 760, 698, 607, 540, 490

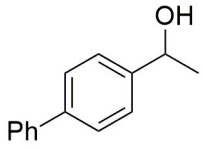

Reaction was performed with 3 mmol of 4-acetylbiphenyl with Ph_2SiH_2 (1.23 mL, 6.6 mmol) and **1** (2.1 mg, $3x10^{-3}$ mmol, 0.1 mol%) in dioxane (1.5 mL). Isolated yield: 544.4 mg (2.76 mmol, 92%). ^1H NMR (400MHz, r.t., $CDCl_3$) δ: 1.55 (d, J = 6.9 Hz, 3H, CH_3), 1.81 (brs, 1H, OH), 4.96 (q, 1H, J = 6.9 Hz, CH), 7.33-7.37 (m, 1H, C_6H_5), 7.42-7.47 (m,

4H, Ph), 7.58-7.60 (m, 4H, Ph). ^{13}C NMR (100MHz, r.t., $CDCl_3$) δ: 25.3 (CH_3), 70.4 (CH), 126.0 (Ph), 127.3 (Ph), 127.4 (Ph), 128.9 (Ph), 140.6 (Ph), 141.0 (Ph), 144.9 (Ph). IR (ATR): 3302, 3095, 3063, 3032, 2990, 2972, 2928, 2884, 1592, 1566, 1484, 1451, 1429, 1404, 1364, 1332, 1291, 1218, 1193, 1183, 1168, 1123, 1085, 1069, 1039, 1022, 1014, 1005, 945, 894, 835, 759, 740, 726, 696, 688, 604, 564, 506.

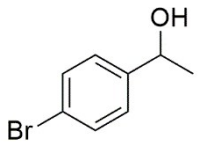

Isolated yield: 180.7 mg (0.90 mmol, 90%). ^{1}H NMR (400MHz, r.t., $CDCl_3$) δ: 1.47 (d, 3H, J = 6.4 Hz, CH_3), 4.88 (q, H, J = 6.4 Hz, CH), 7.23-7.28 (m, 2H, C_6H_4), 7.45-7.49 (m, 2H, C_6H_4). ^{13}C NMR (100MHz, r.t., $CDCl_3$) δ: 25.4 (CH_3), 69.9 (CH), 121.3 (C_6H_4), 127.3 (C_6H_4), 131.7 (C_6H_4), 144.9 (C_6H_4). IR (ATR): 3339, 2972, 2927, 2882, 1901, 1593, 1489, 1447, 1403, 1370, 1338, 1295, 1201, 1112, 1085, 1073, 1009, 898, 824, 772, 716, 537.

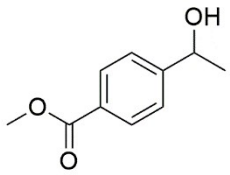

Reaction was performed in dioxane (0.5 mL). Isolated yield: 139.2 mg (0.77 mmol, 77%). ^{1}H NMR (400MHz, r.t., $CDCl_3$) δ: 1.51 (d, 3H, J = 6.9 Hz, CH_3), 1.69 (brs, 1H, OH, overlapped with water), 3.91 (s, 3H, OCH_3), 4.96 (q, H, J = 6.9 Hz, CH), 7.42-7.47 (m, 2H, C_6H_4), 7.99-8.05 (m, 2H, C_6H_4). ^{13}C NMR (100MHz, r.t., $CDCl_3$) δ: 25.5 (CH_3), 52.3 (OCH_3), 70.2 (CH), 125.4 (C_6H_4), 129.4 (C_6H_4), 130.0 (C_6H_4), 151.0 (C_6H_4), 167.1 (CO). IR (ATR): 3420, 3070, 2954, 1716, 1612, 1576, 1436, 1429, 1370, 1311, 1278, 1193, 1178, 1116, 1089, 1068, 1018, 965, 898, 857, 775, 740, 706, 524, 508, 481.

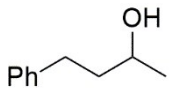

Isolated yield: 124.5 mg (0.83 mmol, 83%). ^{1}H NMR (400MHz, r.t., $CDCl_3$) δ: 1.23 (d, 3H, J = 6.4 Hz, CH_3), 1.48 (brs, 1H, OH), 1.78 (m, 2H, CH_2), 2.72 (m, 2H, $PhCH_2$), 3.83 (sext, 1H, J = 6.4 Hz, CH), 7.19-7.22 (m, 3H, C_6H_5), 7.29 (m, 2H, C_6H_5). ^{13}C NMR (400MHz, r.t., $CDCl_3$) δ: 23.79 (CH_3), 32.28 (CH_2), 41.00 (CH_2), 67.68 (CH), 125.97 (C_6H_5), 128.54 (C_6H_5), 142.17 (C_6H_5). IR (ATR): 3351, 3087, 3062, 3027, 2966, 2927, 2862, 1603, 1496, 1454, 1429, 1374, 1180, 1128, 1082, 1055, 1031, 1000, 954, 935, 906, 856, 745, 698, 578, 527, 479.

Hydrosilylation of cyclohexanone

Catalyst **1** (2.1 mg, $3x10^{-3}$ mmol, 0.1 mol%) was placed in a 10 mL flask, then the mixture of cyclohexanone (310.5 μL, 3 mmol) and Ph_2SiH_2 (1.23 mL, 6.6 mmol) was added. The resulting mixture was stirred for 4 h at r.t., then complete consumption of the substrate was confirmed by ^{1}H NMR spectrum. The yield of the product was determined by ^{1}H NMR spectrum by using hexamethylbenzene as an internal standard.

Deoxygenation of 4-methoxyacetophenone

Catalyst **1** (3.5 mg, 0.005 mmol, 0.5 mol%) was placed in a 10 mL flask, then 4'-methoxyacetophenone (150.2 mg, 1 mmol) and Ph_2SiH_2 (556.8 μL, 3.0 mmol) were added. The resulting mixture was stirred for 1 h at r.t., then complete consumption of the substrate was confirmed by ^{1}H NMR spectrum. The yield of the product was determined by ^{1}H NMR spectrum by using hexamethylbenzene as an internal standard.

Deoxygenation of 4'-methoxyacetophenone catalyzed by *in-situ*-generated catalyst.

KO^{t}Bu (2.2 mg, 0.02 mmol) was added to the solution of $Si(SiMe_3)_4$ (6.4 mg, 0.02 mmol) in tetrahydropyran (0.5 mL) in a 20 mL flask. The solution was stirred at room temperature for 10 min, and $FeBr_2$ (2.2 mg, 0.01 mmol) was added to a solution. The color of the solution turned from pale yellow to greenish brown. The mixture was added to the solution of 4'-methoxyacetophenone (150.2 mg, 1.0 mmol) and Ph_2SiH_2 (553 mg, 3.0 mmol) in a 20 mL flask. The resulting mixture was stirred for 1 h or 24 h at r.t. Hexamethylbenzene (16.2 mg, 0.1 mmol) was added as an internal standard, then the yield of the formed 4-ethylanisole was determined by ^{1}H NMR spectrum. Yield of the product: 53% (1h), 76% (24h)

General Procedure for the Catalytic Silylation of N_2 catalyzed by 1. The following procedure is analogous to those reported in the previous papers.[2] A 20 mL flask was charged with KC_8 (270 mg, 2.0 mmol) and solvent (5 mL), then complex **1** (0.004 mmol, 0.2 mol%) and Me_3SiCl (0.25 mL, 2.0 mmol) was added to this suspension. The remaining suspension was vigorously stirred at room temperature for 24 h under successive supply of N_2 (1 atm). After the reaction, cyclododecane (60 mg, 0.36 mmol) was added as an internal standard, then the yield of the formed $N(SiMe_3)_3$ was determined by GC/GC−MS.

Figure S1. ^{1}H NMR spectrum of solution of **1** in C_6D_6 at room temperature.

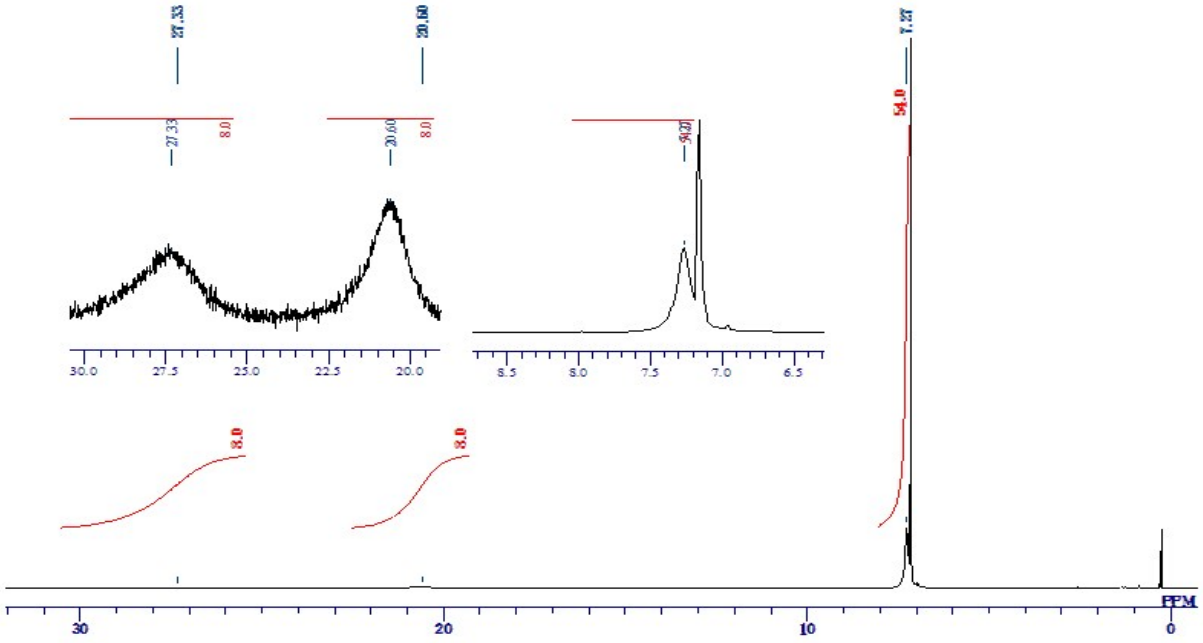

Figure S2. ^{1}H NMR spectrum of **2** in C_6D_6 at room temperature.

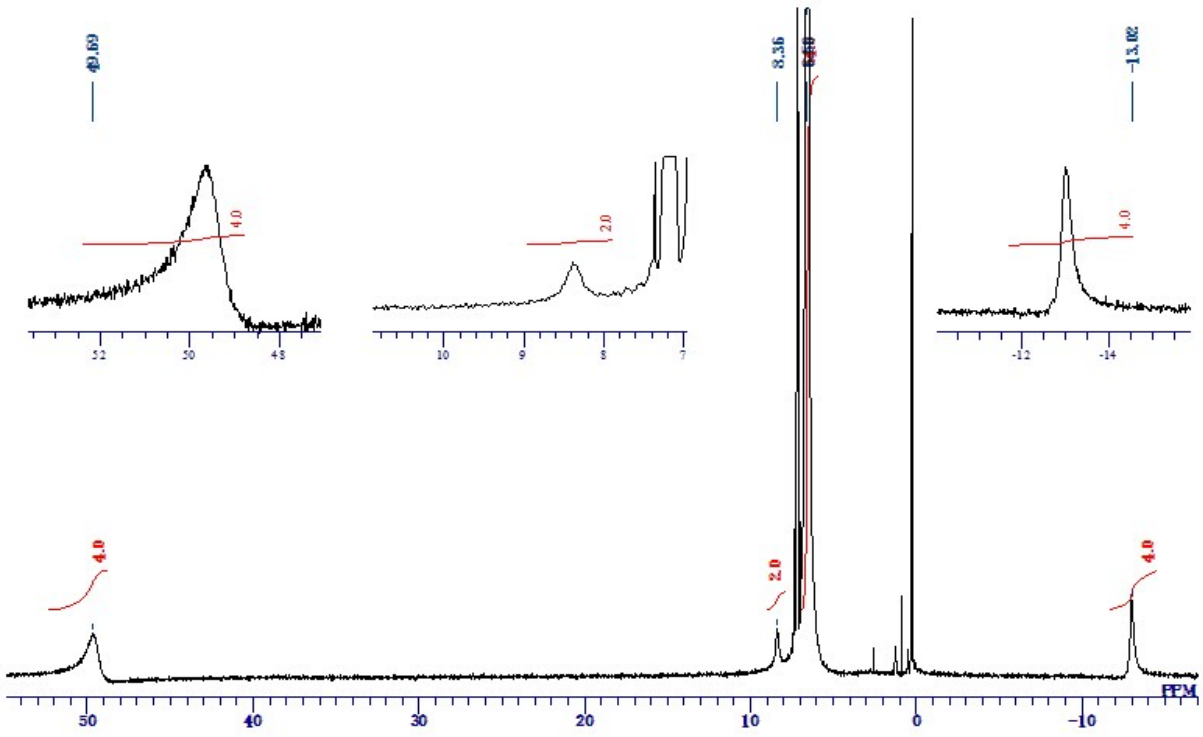

Figure S3-1. ^{1}H NMR spectrum of the crude product obtained from the reaction of **1** with 2 equiv. of pyridine in C_6D_6 at room temperature.

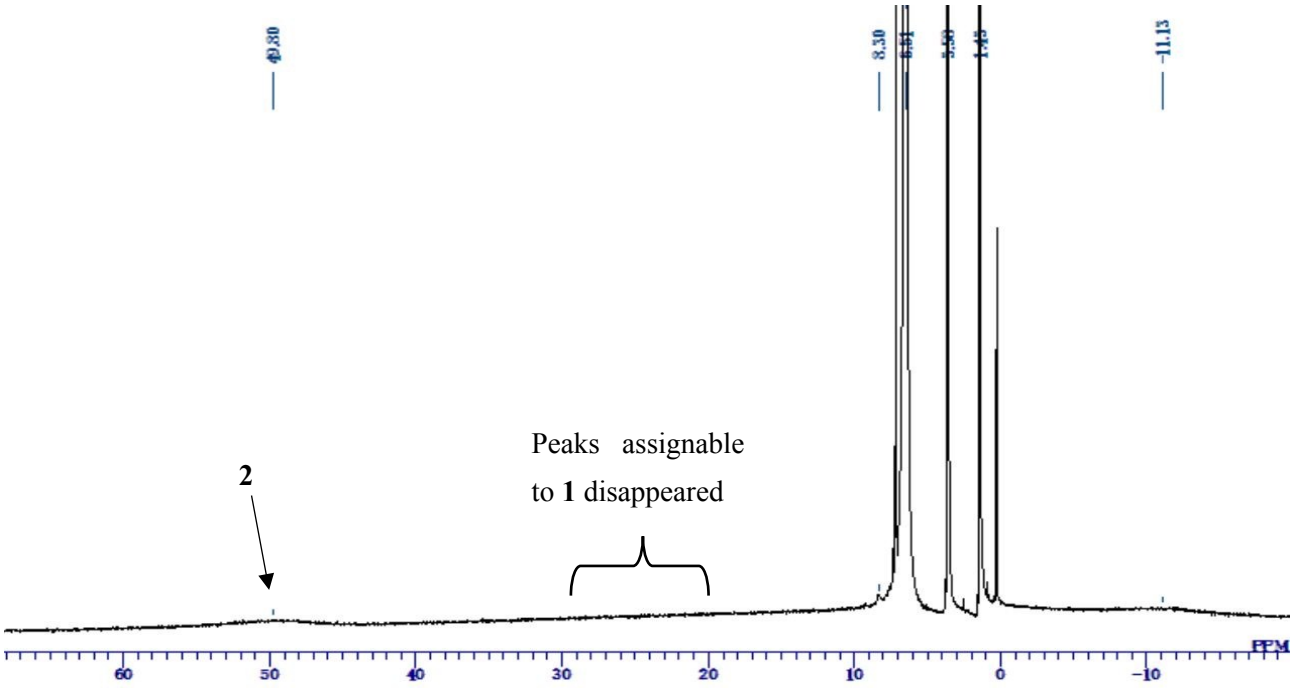

Figure S3-2. ^{1}H NMR spectrum (5-9 ppm) of **1**(isolated) in C_6D_6 at room temperature (top), the crude product obtained from the reaction of **1** with 2 equiv. of pyridine in C_6D_6 at room temperature (middle), and **2**(isolated) in C_6D_6 at room temperature (bottom).

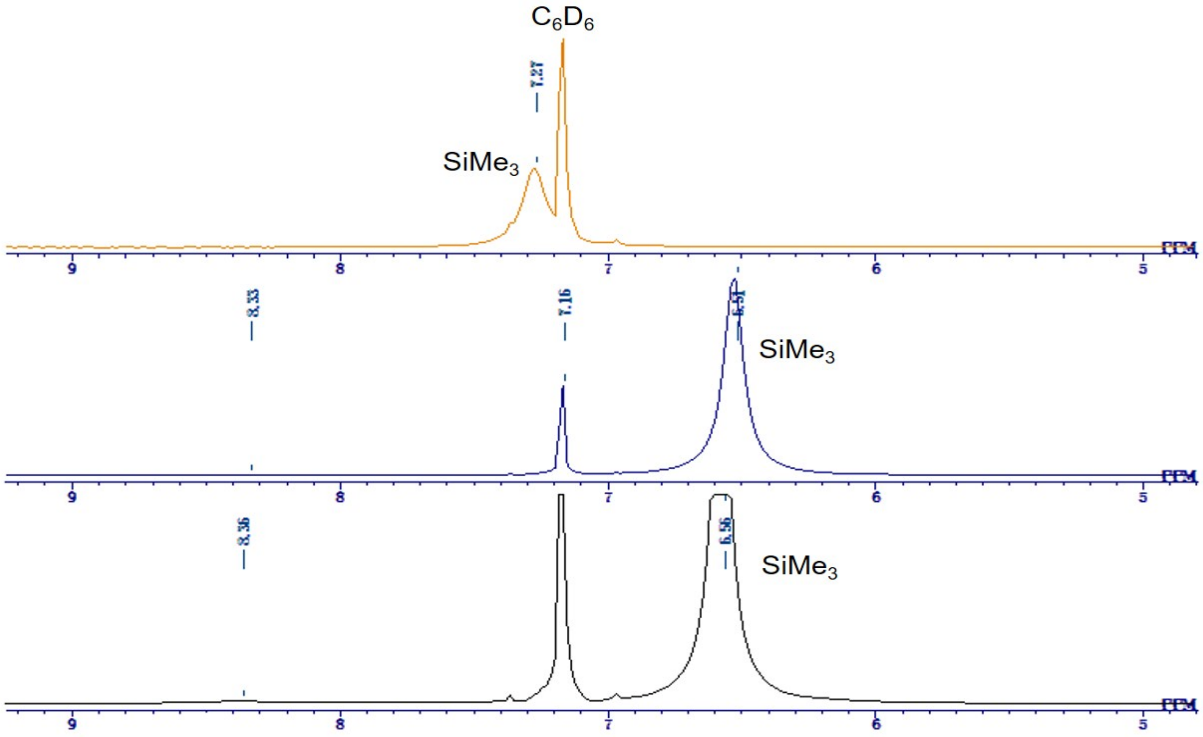

Figure S4-1. ^{1}H NMR spectrum of benzyl acetate in $CDCl_3$ at room temperature.

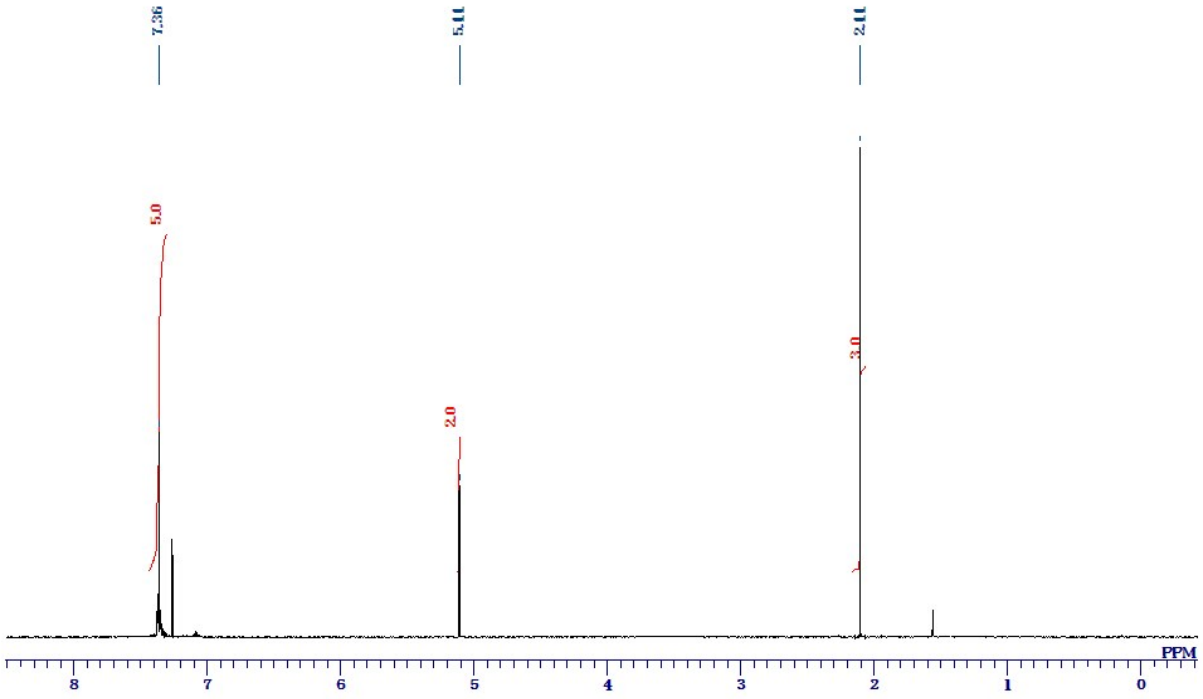

Figure S4-2. ^{13}C NMR spectrum of benzyl acetate in $CDCl_3$ at room temperature.

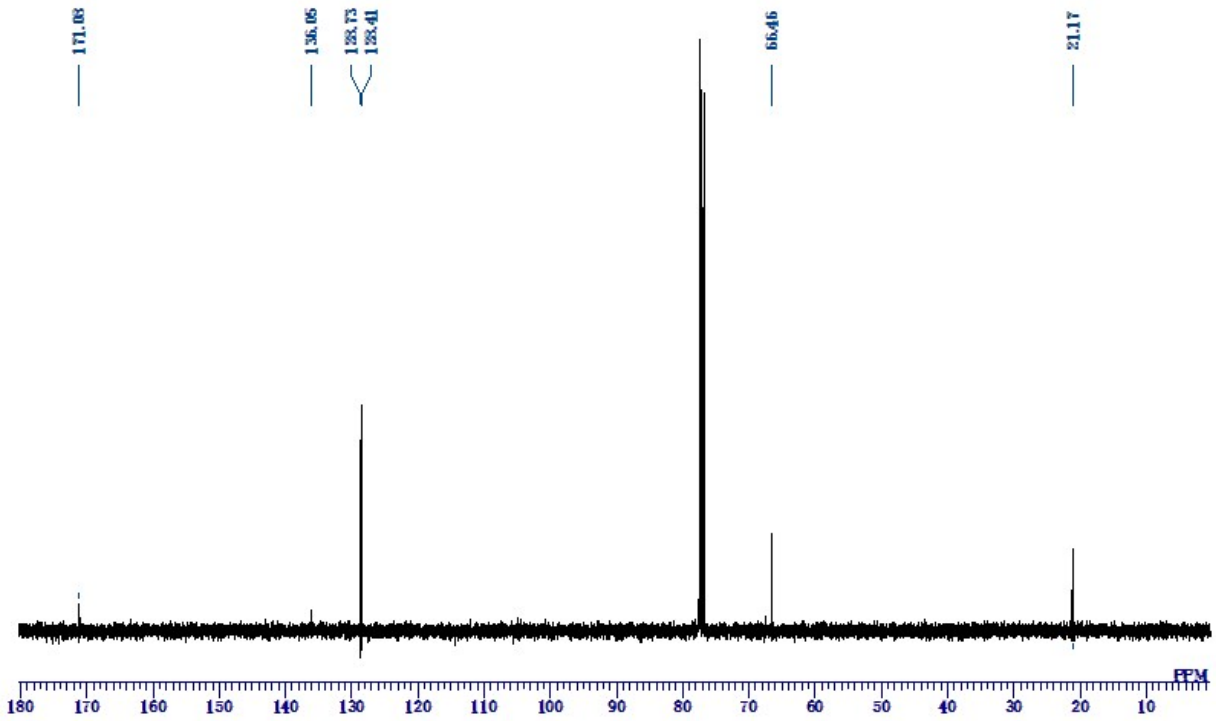

Figure S5-1. ^{1}H NMR spectrum of 3-Phenyl-1-propanol in $CDCl_3$ at room temperature.

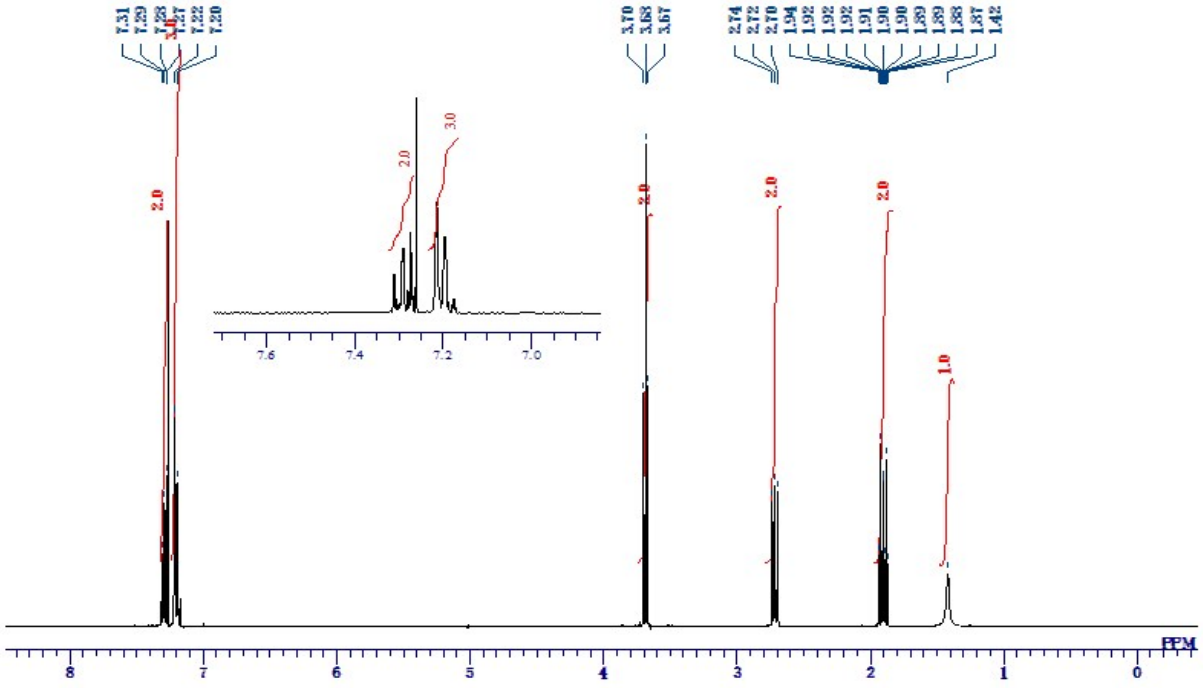

Figure S5-2. ^{13}C NMR spectrum of 3-Phenyl-1-propanol in $CDCl_3$ at room temperature.

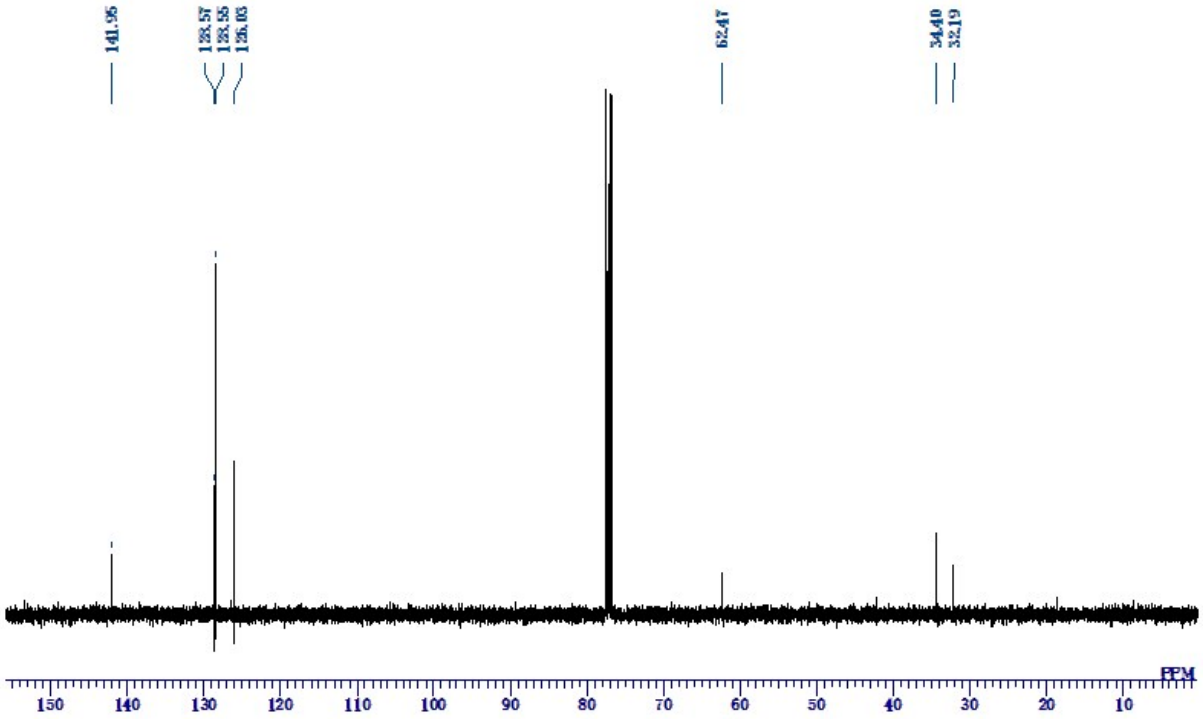

Figure S6-1. ^{1}H NMR spectrum of 1-phenylethanol in $CDCl_3$ at room temperature.

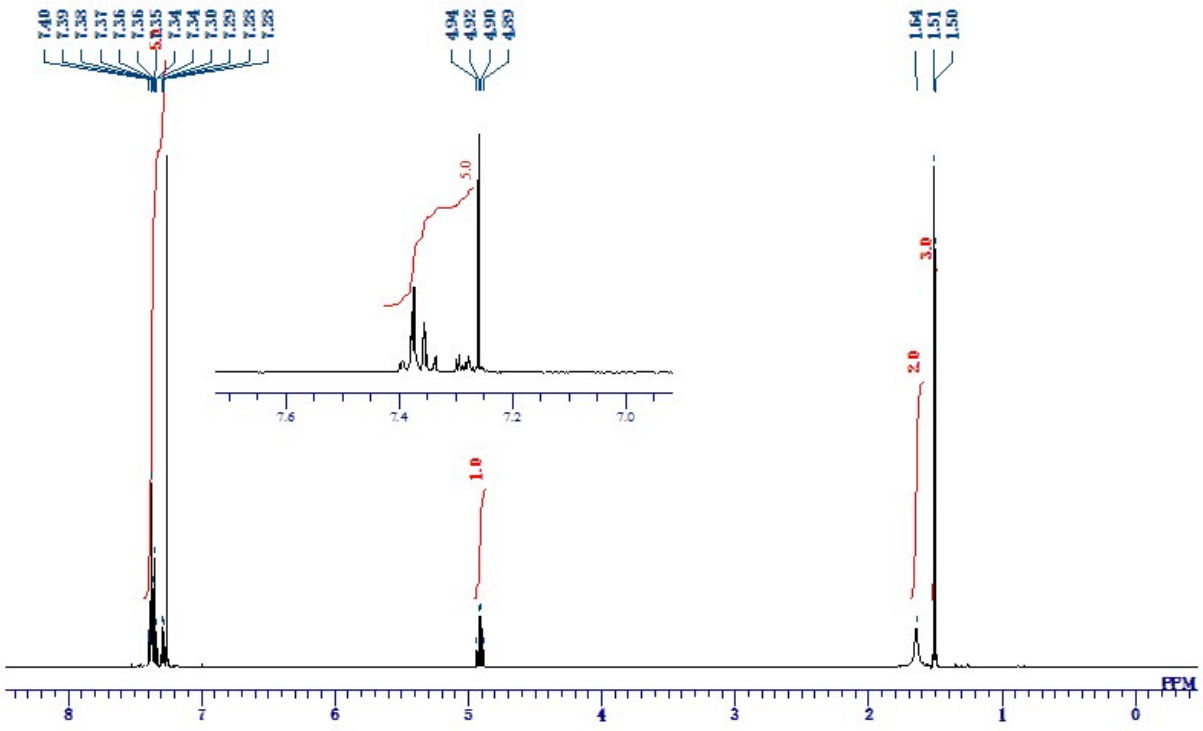

Figure S6-2. ^{13}C NMR spectrum of 1-phenylethanol in $CDCl_3$ at room temperature.

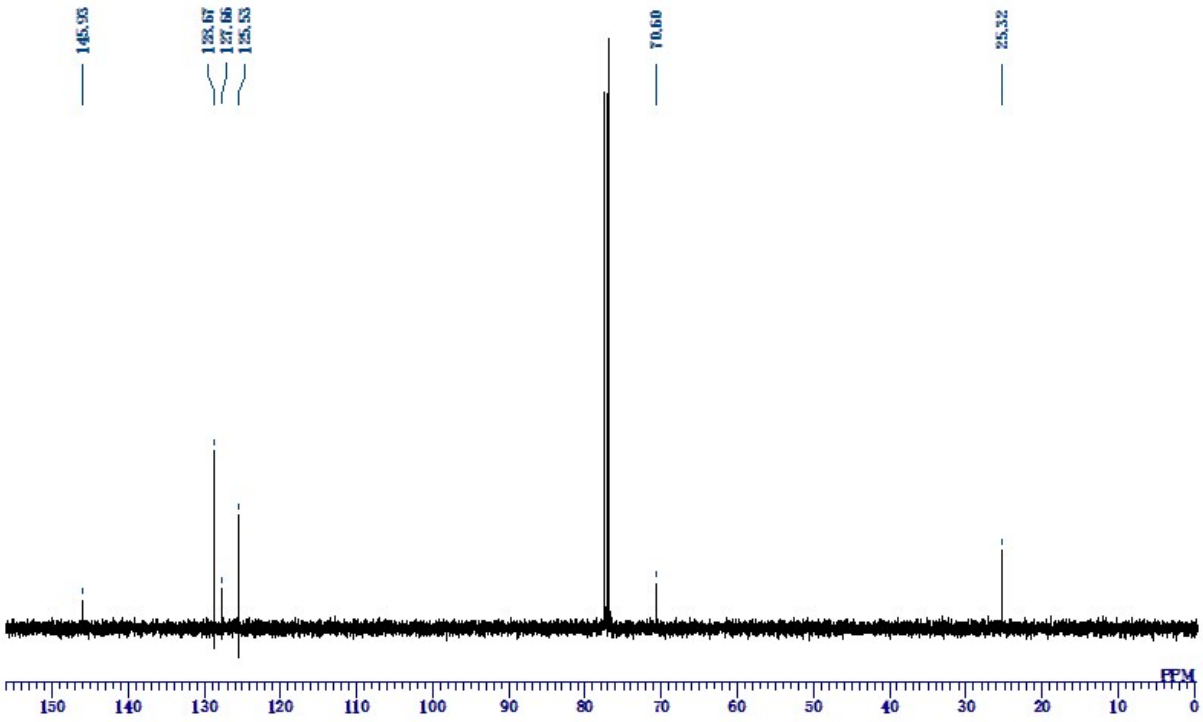

Figure S7-1. ^{1}H NMR spectrum of 4-(1-hydroxyethyl)biphenyl in $CDCl_3$ at room temperature.

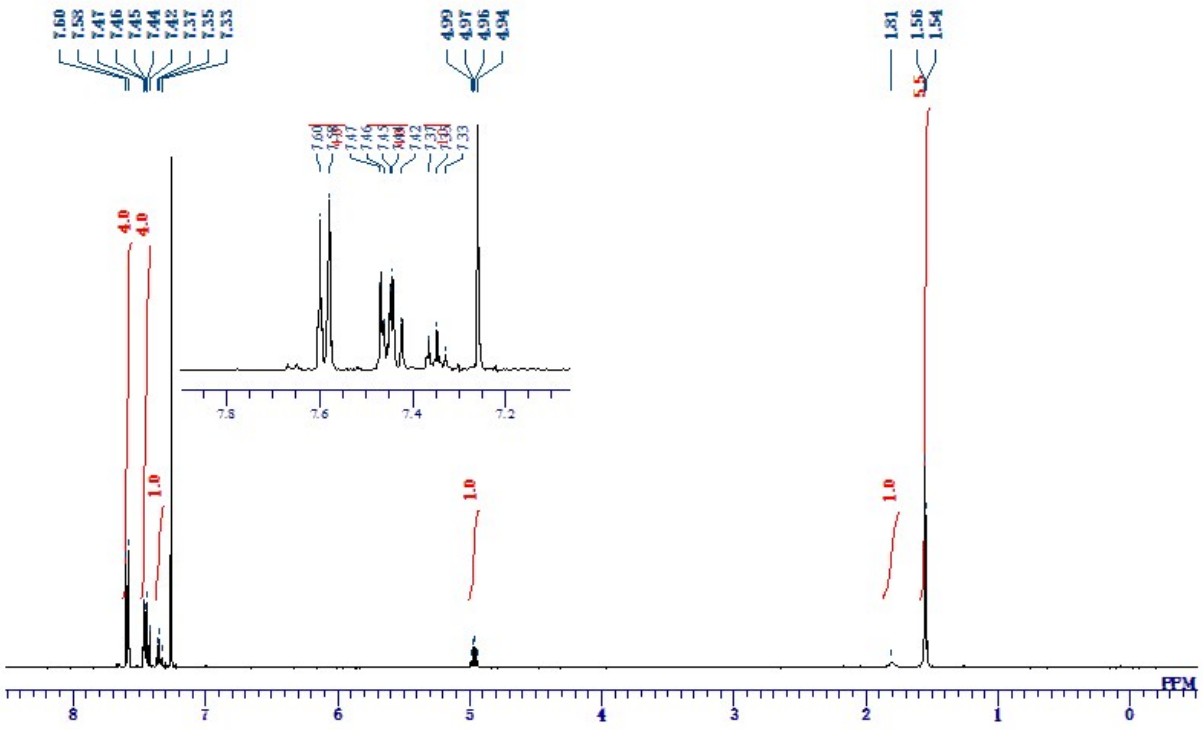

Figure S7-2. ^{13}C NMR spectrum of 4-(1-hydroxyethyl)biphenyl in $CDCl_3$ at room temperature.

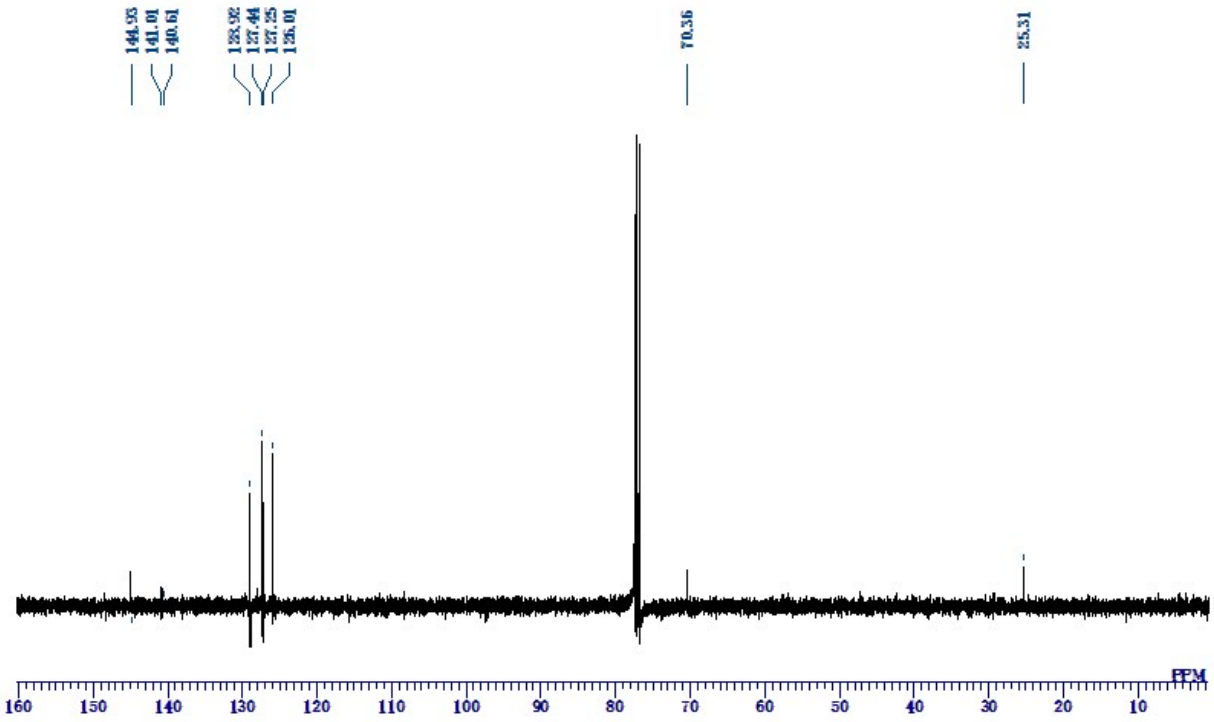

Figure S8-1. ^{1}H NMR spectrum of 1-(4-bromophenyl)ethanol in $CDCl_3$ at room temperature.

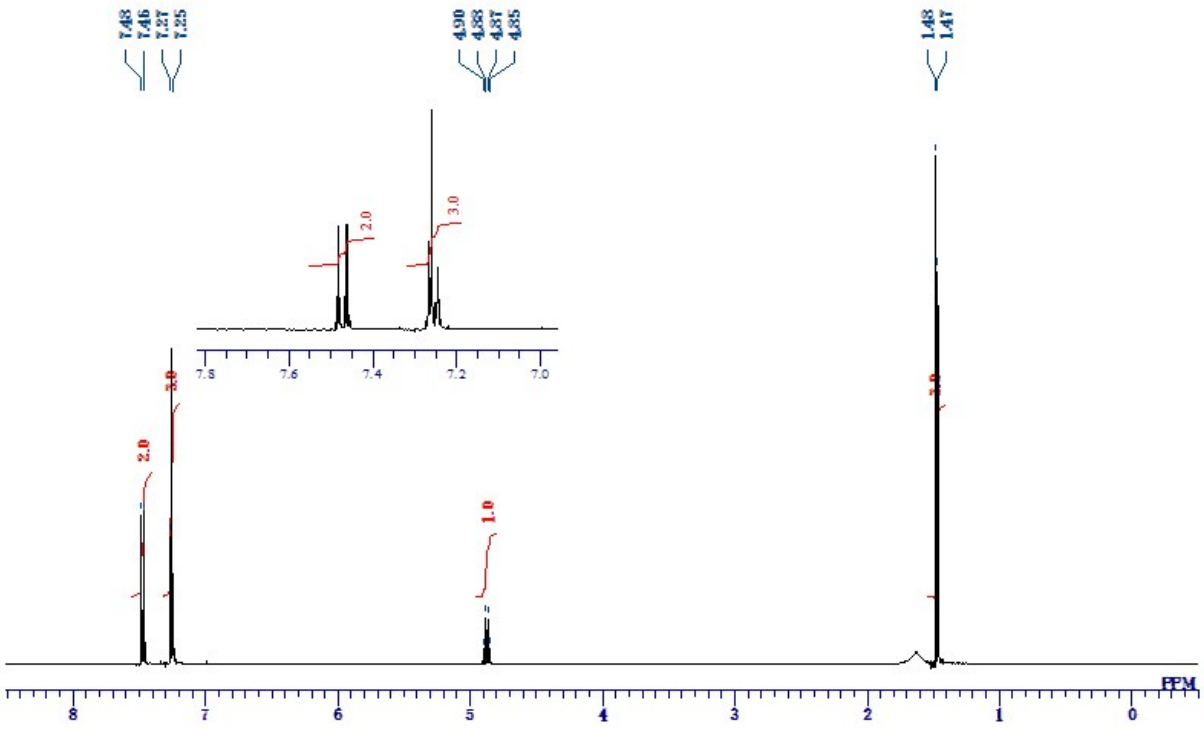

Figure S8-2. ^{13}C NMR spectrum of 1-(4-bromophenyl)ethanol in $CDCl_3$ at room temperature.

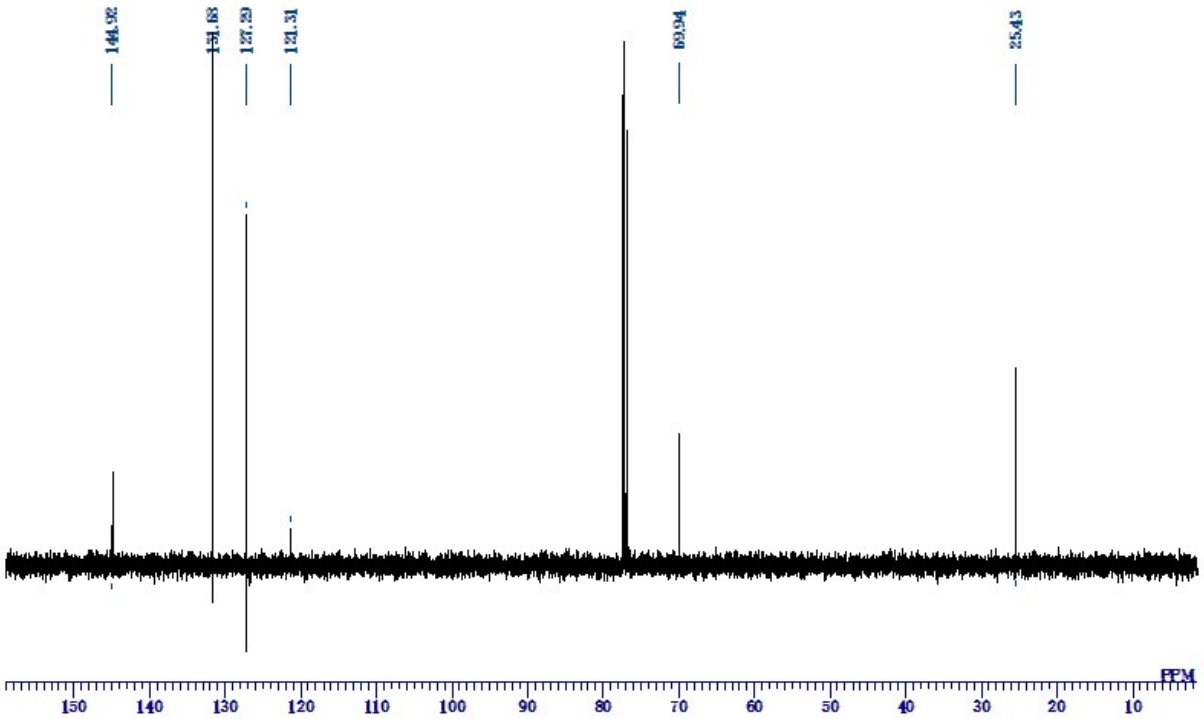

Figure S9-1. ^{1}H NMR spectrum of methyl 4-(1-hydroxyethyl)benzoate in $CDCl_3$ at room temperature.

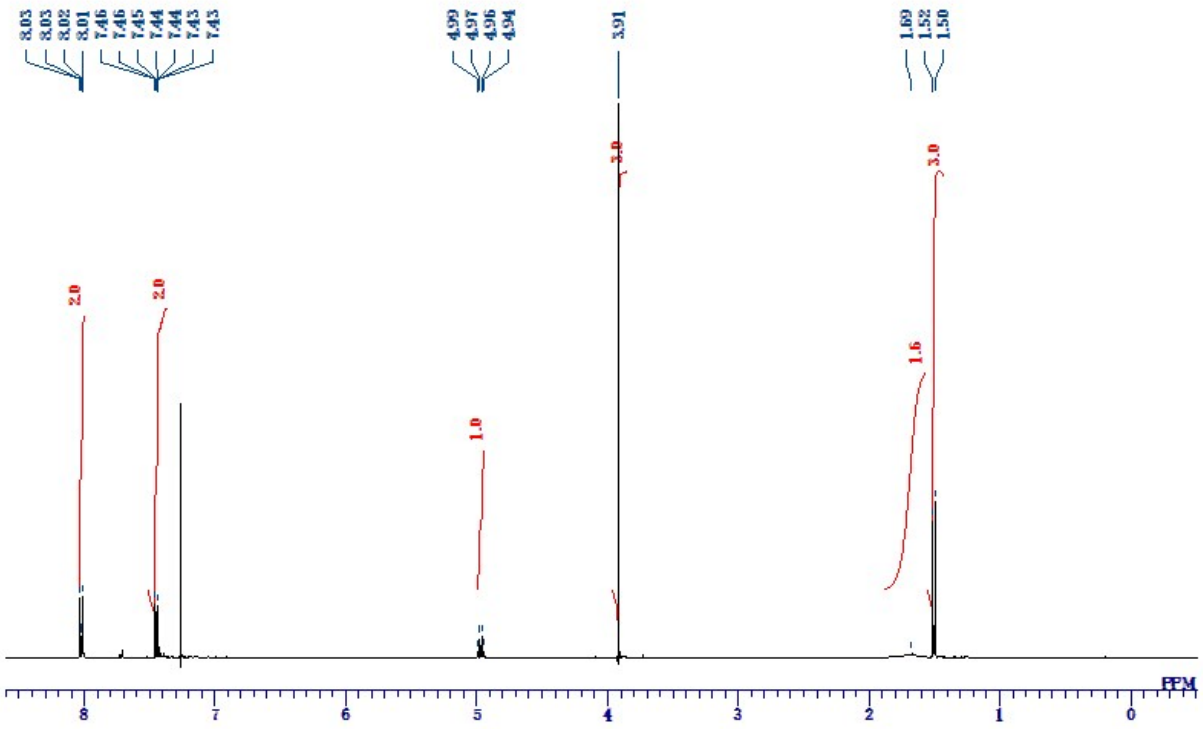

Figure S9-2. ^{13}C NMR spectrum of methyl 4-(1-hydroxyethyl)benzoate in $CDCl_3$ at room temperature.

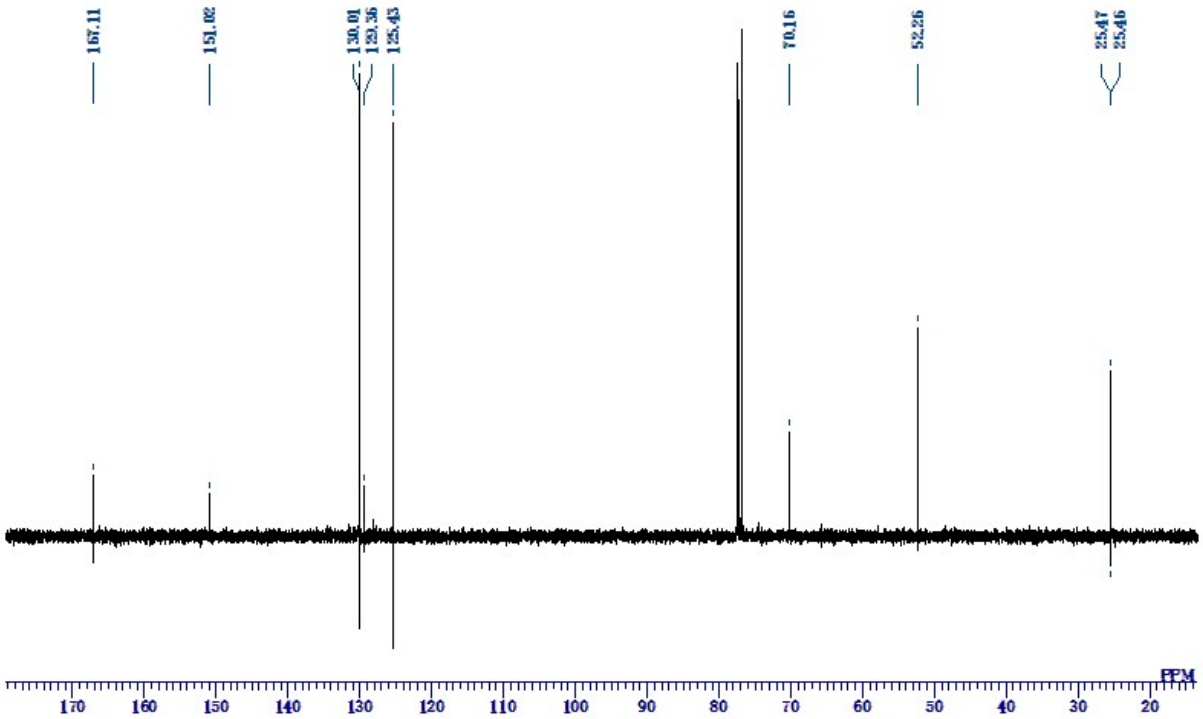

Figure S10-1. ^{1}H NMR spectrum of 4-phenyl-2-butanol in $CDCl_3$ at room temperature.

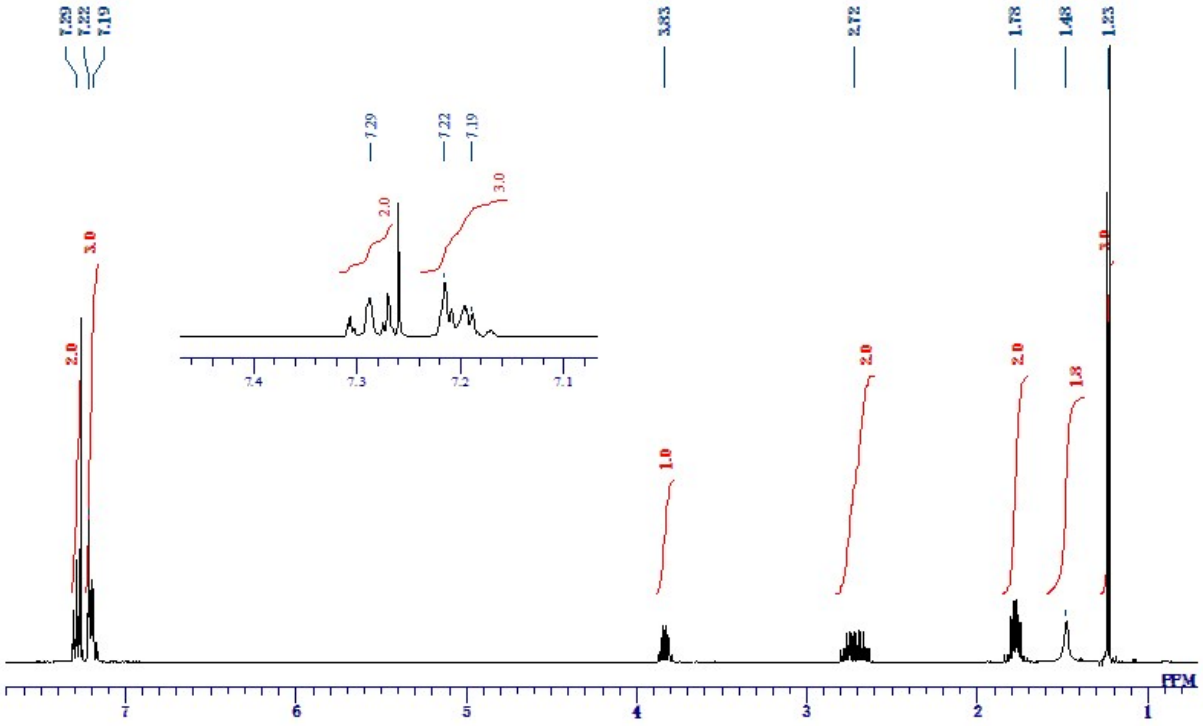

Figure S10-2. ^{13}C NMR spectrum of 4-phenyl-2-butanol in $CDCl_3$ at room temperature.

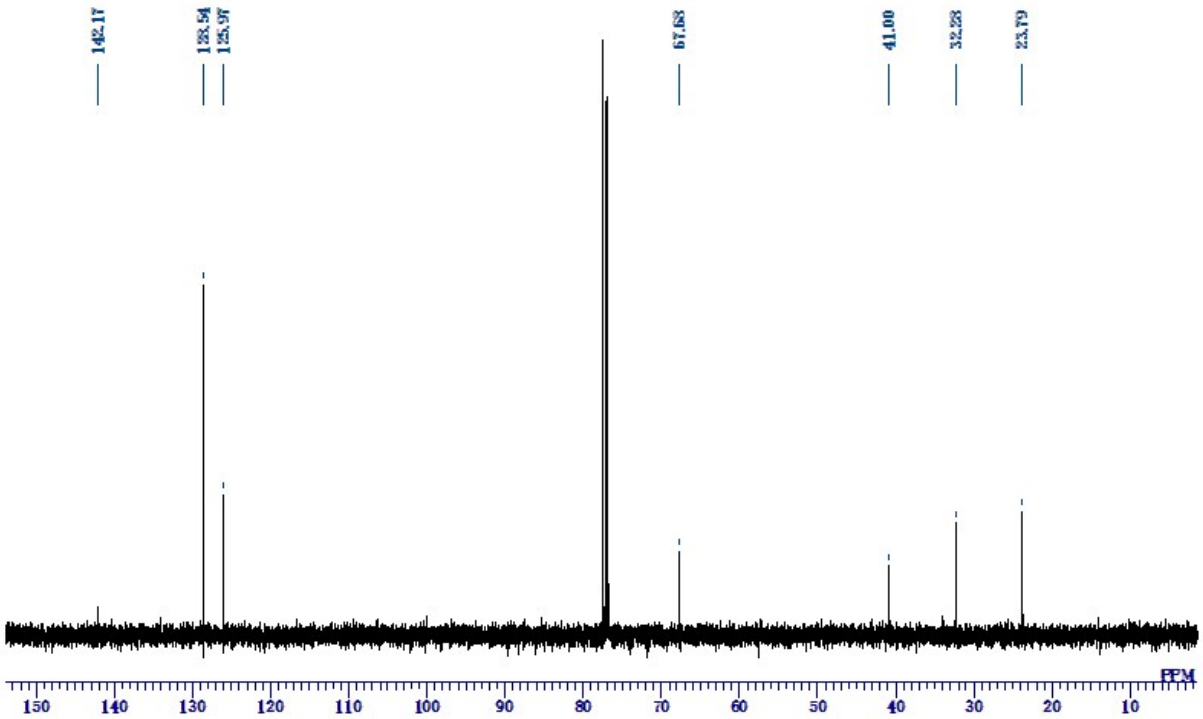

Figure S11. ^{1}H NMR spectrum of the crude product obtained from the reation of 4'-methoxyacetophenone with Ph_2SiH_2 catalyzed by **1** in $CDCl_3$ at room temperature (top), ^{1}H NMR spectrum of the commercially available authentic 4-ethylanisole in $CDCl_3$ at room temperature (bottom). Yield was determined by using hexamethylbenzene as an internal standard.

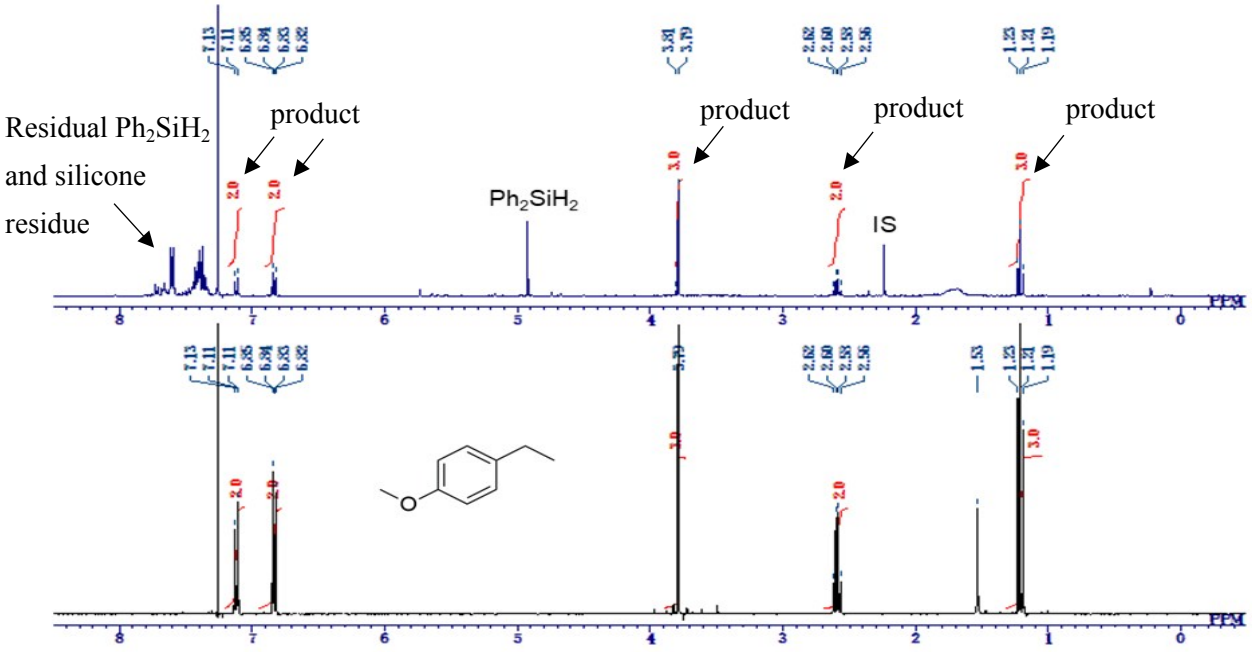

Figure S12. ^{1}H NMR spectrum of the product obtained from the reaction of cyclohexanone with Ph_2SiH_2 catalyzed by **1** in $CDCl_3$ at room temperature. Yield was determined by using hexamethylbenzene as an internal standard.

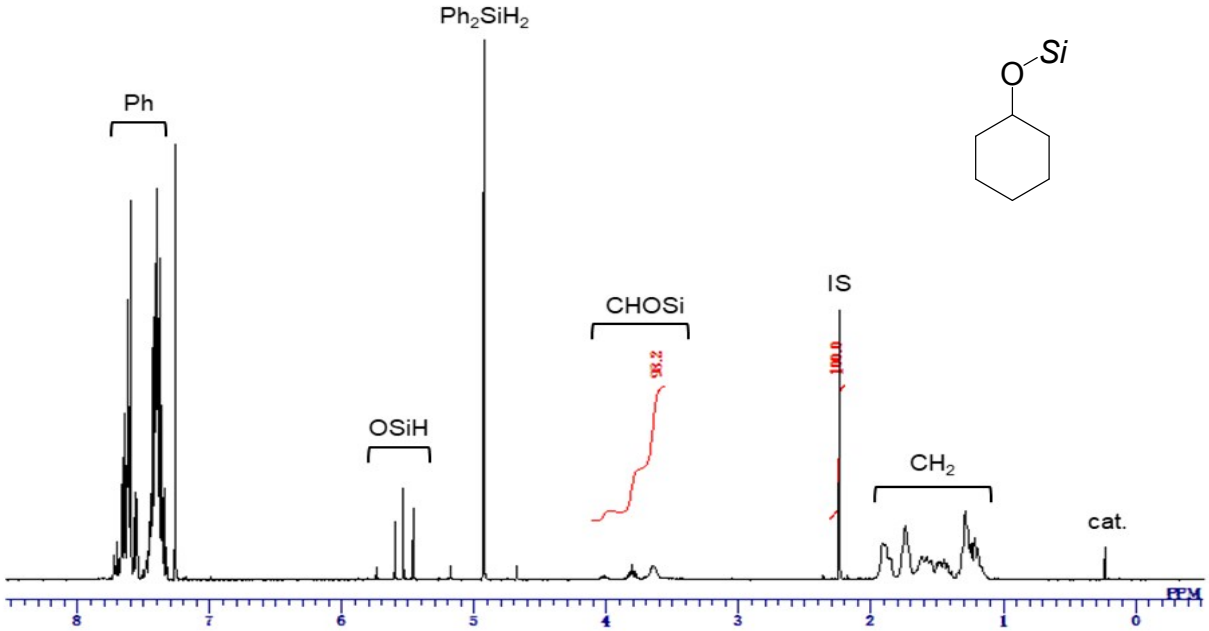

X-ray data collection and reduction

X-ray crystallography was performed on a Rigaku Saturn CCD area detector with graphite monochromated Mo-Kα radiation (λ=0.71075 Å). The data were collected at 183(2) K using ω scan in the θ range of $3.00 \leq \theta \leq 27.49$ deg (**1**) and $3.06 \leq \theta \leq 27.49$ deg (**2**). The data obtained were processed using Crystal-Clear (Rigaku) on a Pentium computer, and were corrected for Lorentz and polarization effects. The structures were solved by direct methods[3], and expanded using Fourier techniques. Hydrogen atoms were refined using the riding model. The final cycle of full-matrix least-squares refinement on F^2 was based on 5663 observed reflections and 200 variable parameters for **1**, 9756 observed reflections and 352 variable parameters for **2**. Neutral atom scattering factors were taken from International Tables for Crystallography (IT), Vol. C, Table 6.1.1.4[4]. Anomalous dispersion effects were included in Fcalc[5]; the values for Δf' and Δf'' were those of Creagh and McAuley[6]. The values for the mass attenuation coefficients are those of Creagh and Hubbell[7]. All calculations were performed using the CrystalStructure[8] crystallographic software package except for refinement, which was performed using SHELXL Version 2017/1[9].Details of final refinement as well as the bond lengths and angle are summarized in Tables S1 and S2, and the numbering scheme employed is also shown in Figures S13 and 14 which were drawn with ORTEP at 50% probability ellipsoids.

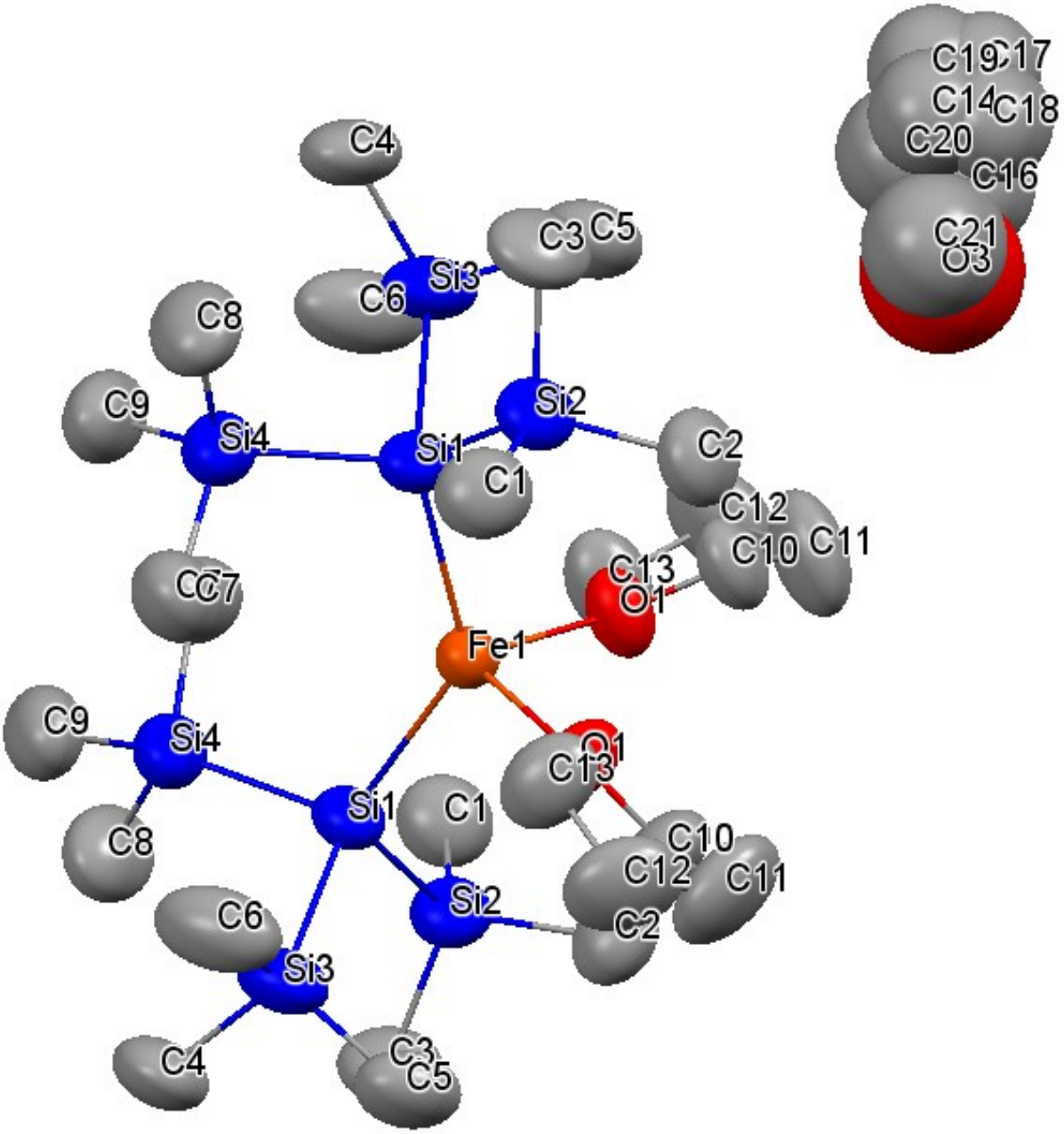

Figure S13. ORTEP drawing of **1** (50% probability of the thermal ellipsoids)

Table S1-1. Crystal data and structure refinement for **1**.

Empirical Formula	$C_{34}H_{70}FeO_4Si_8$
Formula Weight	823.46
Crystal Color, Habit	pueple, prism
Crystal Dimensions	0.300 X 0.200 X 0.100 mm
Crystal System	monoclinic
Lattice Type	Primitive
Lattice Parameters	a = 13.790(3) Å
	b = 10.428(2) Å
	c = 18.950(5) Å
	β = 111.077(4) ^{o}
	V = 2542.7(10) Å^3
Space Group	P2/c (#13)
Z value	2
D_{calc}	1.075 g/cm^3
F_{000}	888.00
μ(MoKα)	5.134 cm^{-1}
Diffractometer	Saturn724
Radiation	MoKα (λ = 0.71075 Å)
	multi-layer mirror monochromated
Voltage, Current	50kV, 24mA
Temperature	-89.8^{o}C
Detector Aperture	72.8 x 72.8 mm
Data Images	720 exposures
ω oscillation Range (χ=45.0, ϕ=0.0)	-70.0 - 110.0^o
Exposure Rate	10.0 sec./^{o}
Detector Swing Angle	19.97^o
ω oscillation Range (χ=45.0, ϕ=90.0)	-70.0 - 110.0^o
Exposure Rate	10.0 sec./^{o}
Detector Swing Angle	19.97^o
Detector Position	44.82 mm
Pixel Size	0.141 mm
$2\theta_{max}$	55.0^o
No. of Reflections Measured	Total: 20592
	Unique: 5663 (R_{int} = 0.0358)
Corrections	Lorentz-polarization
	Absorption
	(trans. factors: 0.841 - 0.950)
Structure Solution	Direct Methods (SIR2008)

Refinement	Full-matrix least-squares on F^2
Function Minimized	Σ w $(Fo^2 - Fc^2)^2$
Least Squares Weights	$w = 1/ [\sigma^2(Fo^2) + (0.0783 \cdot P)^2 + 1.1831 \cdot P]$ where $P = (Max(Fo^2,0) + 2Fc^2)/3$
$2\theta_{max}$ cutoff	54.9^o
Anomalous Dispersion	All non-hydrogen atoms
No. Observations (All reflections)	5663
No. Variables	200
Reflection/Parameter Ratio	28.32
Residuals: R1 (I>2.00σ(I))	0.0513
Residuals: R (All reflections)	0.0634
Residuals: wR2 (All reflections)	0.1458
Goodness of Fit Indicator	1.071
Max Shift/Error in Final Cycle	0.001
Maximum peak in Final Diff. Map	0.95 $e^-/Å^3$
Minimum peak in Final Diff. Map	-0.78 $e^-/Å^3$

Table S1-2. Atomic coordinates and B_{iso}/B_{eq}

atom	x	y	z	B_{eq}	
Fe1	0.50000	0.88335(4)	0.25000	2.096(11)	1/2
Si1	0.31841(5)	0.97628(6)	0.21698(4)	2.476(13)	1
Si2	0.18218(5)	0.85507(7)	0.13095(4)	2.883(14)	1
Si3	0.26501(6)	1.00440(8)	0.32095(4)	3.318(16)	1
Si4	0.29258(6)	1.18051(7)	0.16088(5)	3.355(16)	1
O1	0.50606(14)	0.73847(17)	0.32890(9)	3.00(3)	1
O3	0.2343(5)	0.4777(6)	0.4029(4)	14.50(17)	1
C1	0.1663(2)	0.8870(3)	0.02911(15)	4.04(6)	1
C2	0.2037(2)	0.6772(3)	0.14701(17)	4.06(6)	1
C3	0.0502(2)	0.8871(3)	0.13596(18)	4.34(6)	1
C4	0.1502(2)	1.1141(3)	0.3014(2)	4.63(7)	1
C5	0.2270(3)	0.8495(4)	0.35464(19)	4.72(7)	1
C6	0.3703(3)	1.0775(4)	0.40455(18)	5.59(9)	1
C7	0.3585(3)	1.1906(4)	0.0902(2)	4.99(7)	1
C8	0.1525(3)	1.2266(3)	0.1098(2)	5.03(7)	1
C9	0.3490(3)	1.3112(3)	0.2322(2)	5.10(7)	1
C10	0.4362(2)	0.6305(3)	0.31733(16)	3.59(5)	1
C11	0.4771(3)	0.5561(4)	0.38881(19)	5.61(8)	1
C12	0.5172(3)	0.6605(4)	0.44866(17)	5.26(8)	1
C13	0.5541(3)	0.7622(3)	0.40938(15)	4.15(6)	1
C14	0.0616(10)	0.5182(13)	0.3528(7)	8.6(3)	1/2
C16	0.2148(10)	0.4679(13)	0.4642(7)	8.5(3)	1/2
C17	0.0884(9)	0.4771(11)	0.4352(6)	6.7(2)	1/2
C18	0.0587(9)	0.4523(12)	0.3531(6)	7.7(3)	1/2
C19	0.1019(12)	0.5316(14)	0.4380(8)	9.1(4)	1/2
C20	0.2024(12)	0.5454(16)	0.4694(8)	10.1(4)	1/2
C21	0.1521(6)	0.4875(7)	0.3331(5)	11.40(19)	1

$B_{eq} = 8/3\ \pi^2(U_{11}(aa^*)^2 + U_{22}(bb^*)^2 + U_{33}(cc^*)^2 + 2U_{12}(aa^*bb^*)\cos\gamma + 2U_{13}(aa^*cc^*)\cos\beta + 2U_{23}(bb^*cc^*)\cos\alpha)$

Table S1-3. Anisotropic displacement parameters

atom	U_{11}	U_{22}	U_{33}	U_{12}	U_{13}	U_{23}
Fe1	0.0260(2)	0.0280(2)	0.0256(3)	0.00000	0.00928(19)	0.00000
Si1	0.0233(3)	0.0378(4)	0.0317(4)	-0.0010(2)	0.0084(3)	-0.0045(3)

Si2	0.0265(3)	0.0451(4)	0.0335(4)	-0.0040(3)	0.0054(3)	-0.0032(3)
Si3	0.0298(4)	0.0609(5)	0.0377(4)	-0.0029(3)	0.0149(3)	-0.0114(3)
Si4	0.0350(4)	0.0373(4)	0.0551(5)	0.0013(3)	0.0162(4)	-0.0001(3)
O1	0.0474(10)	0.0383(9)	0.0243(9)	-0.0107(8)	0.0080(7)	0.0037(7)
C1	0.0449(16)	0.064(2)	0.0362(15)	0.0020(13)	0.0049(13)	-0.0009(13)
C2	0.0525(17)	0.0474(16)	0.0475(17)	-0.0117(13)	0.0098(14)	-0.0054(13)
C3	0.0277(13)	0.075(2)	0.0570(19)	-0.0096(13)	0.0091(13)	-0.0073(15)
C4	0.0452(17)	0.068(2)	0.074(2)	0.0028(14)	0.0350(17)	-0.0098(16)
C5	0.0543(18)	0.078(2)	0.0558(19)	0.0044(16)	0.0306(16)	0.0091(17)
C6	0.0480(18)	0.117(3)	0.0484(19)	-0.015(2)	0.0188(15)	-0.030(2)
C7	0.066(2)	0.058(2)	0.074(2)	-0.0015(16)	0.0349(18)	0.0083(17)
C8	0.0480(17)	0.057(2)	0.080(2)	0.0137(15)	0.0162(17)	0.0159(17)
C9	0.064(2)	0.0458(18)	0.089(3)	-0.0069(15)	0.0333(19)	-0.0151(17)
C10	0.0515(16)	0.0426(15)	0.0415(15)	-0.0166(12)	0.0158(13)	-0.0006(11)
C11	0.086(3)	0.059(2)	0.059(2)	-0.0192(19)	0.0148(19)	0.0232(17)
C12	0.072(2)	0.091(3)	0.0345(17)	-0.0116(19)	0.0165(16)	0.0155(16)
C13	0.0660(19)	0.0590(18)	0.0263(14)	-0.0166(15)	0.0087(13)	-0.0021(12)

The general temperature factor expression: $\exp(-2\pi^2(a^{*2}U_{11}h^2 + b^{*2}U_{22}k^2 + c^{*2}U_{33}l^2 + 2a^*b^*U_{12}hk + 2a^*c^*U_{13}hl + 2b^*c^*U_{23}kl))$

Table S1-4. Bond lengths (Å)

atom	atom	distance	atom	atom	distance
Fe1	Si1	2.5445(8)	Fe1	Si1[1]	2.5445(8)
Fe1	O1	2.1059(18)	Fe1	O1[1]	2.1059(18)
Si1	Si2	2.3626(9)	Si1	Si3	2.3566(13)
Si1	Si4	2.3495(11)	Si2	C1	1.892(3)
Si2	C2	1.886(3)	Si2	C3	1.886(3)
Si3	C4	1.879(3)	Si3	C5	1.880(4)
Si3	C6	1.883(3)	Si4	C7	1.873(5)
Si4	C8	1.885(3)	Si4	C9	1.880(3)
O1	C10	1.446(4)	O1	C13	1.449(3)
O3	C16	1.286(17)	O3	C20	1.637(19)
O3	C21	1.402(9)	C10	C11	1.485(4)
C11	C12	1.525(5)	C12	C13	1.486(5)
C14	C17	1.531(18)	C14	C18	0.689(19)
C14	C19	1.514(19)	C14	C21	1.461(18)
C16	C17	1.631(17)	C16	C19	1.60(2)

C16	C20	0.84(2)	C17	C18	1.482(16)
C17	C19	0.594(19)	C17	C20	1.632(19)
C18	C19	1.714(19)	C18	C21	1.512(17)
C19	C20	1.30(2)			

Symmetry Operators:
(1) -X+1,Y,-Z+1/2

Table S1-5. Bond angles (°)

atom	atom	atom	angle	atom	atom	atom	angle
Si1	Fe1	Si1[1]	135.23(3)	Si1	Fe1	O1	103.42(6)
Si1	Fe1	O1[1]	108.32(5)	Si1[1]	Fe1	O1	108.32(5)
Si1[1]	Fe1	O1[1]	103.42(6)	O1	Fe1	O1[1]	88.32(7)
Fe1	Si1	Si2	115.72(4)	Fe1	Si1	Si3	114.68(3)
Fe1	Si1	Si4	115.60(4)	Si2	Si1	Si3	103.50(4)
Si2	Si1	Si4	102.66(4)	Si3	Si1	Si4	102.91(4)
Si1	Si2	C1	112.42(10)	Si1	Si2	C2	112.03(9)
Si1	Si2	C3	114.38(11)	C1	Si2	C2	106.95(15)
C1	Si2	C3	105.09(14)	C2	Si2	C3	105.33(16)
Si1	Si3	C4	113.90(13)	Si1	Si3	C5	112.71(13)
Si1	Si3	C6	112.06(13)	C4	Si3	C5	105.80(17)
C4	Si3	C6	105.08(17)	C5	Si3	C6	106.67(16)
Si1	Si4	C7	109.94(12)	Si1	Si4	C8	115.07(12)
Si1	Si4	C9	112.05(12)	C7	Si4	C8	106.85(17)
C7	Si4	C9	106.98(18)	C8	Si4	C9	105.50(16)
Fe1	O1	C10	126.63(14)	Fe1	O1	C13	120.75(17)
C10	O1	C13	108.7(2)	C16	O3	C20	30.5(9)
C16	O3	C21	119.8(8)	C20	O3	C21	110.2(7)
O1	C10	C11	104.7(2)	C10	C11	C12	102.9(3)
C11	C12	C13	103.6(3)	O1	C13	C12	107.2(2)
C17	C14	C18	72.8(15)	C17	C14	C19	22.5(7)
C17	C14	C21	106.4(9)	C18	C14	C19	94.7(17)
C18	C14	C21	80.8(18)	C19	C14	C21	105.8(10)
O3	C16	C17	103.7(9)	O3	C16	C19	100.6(10)
O3	C16	C20	98.5(17)	C17	C16	C19	21.2(7)
C17	C16	C20	75.2(14)	C19	C16	C20	54.5(13)
C14	C17	C16	101.4(11)	C14	C17	C18	26.4(7)
C14	C17	C19	77.2(19)	C14	C17	C20	97.4(10)

C16	C17	C18	101.6(10)	C16	C17	C19	76.4(19)
C16	C17	C20	29.8(8)	C18	C17	C19	103(2)
C18	C17	C20	110.9(11)	C19	C17	C20	47.3(17)
C14	C18	C17	80.8(16)	C14	C18	C19	61.7(15)
C14	C18	C21	72.5(17)	C17	C18	C19	19.8(7)
C17	C18	C21	106.4(9)	C19	C18	C21	94.5(9)
C14	C19	C16	103.6(13)	C14	C19	C17	80.3(18)
C14	C19	C18	23.6(7)	C14	C19	C20	114.8(16)
C16	C19	C17	82.4(19)	C16	C19	C18	93.5(11)
C16	C19	C20	31.6(9)	C17	C19	C18	57.5(17)
C17	C19	C20	113(2)	C18	C19	C20	115.8(15)
O3	C20	C16	51.0(14)	O3	C20	C17	89.6(9)
O3	C20	C19	97.9(11)	C16	C20	C17	75.0(14)
C16	C20	C19	93.9(16)	C17	C20	C19	19.6(8)
O3	C21	C14	104.5(8)	O3	C21	C18	102.6(8)
C14	C21	C18	26.7(8)				

Symmetry Operators:

(1) -X+1,Y,-Z+1/2

Table S1-6. Torsion Angles(°)

(Those having bond angles > 160 or < 20 degrees are excluded.)

atom1	atom2	atom3	atom4	angle	atom1	atom2	atom3	atom4	angle
Si1	Fe1	Si1[1]	Si2[1]	147.20(3)	Si1	Fe1	Si1[1]	Si3[1]	-92.36(4)
Si1	Fe1	Si1[1]	Si4[1]	27.17(5)	Si1[1]	Fe1	Si1	Si2	147.20(3)
Si1[1]	Fe1	Si1	Si3	-92.36(4)	Si1[1]	Fe1	Si1	Si4	27.17(5)
Si1	Fe1	O1	C10	57.25(15)	Si1	Fe1	O1	C13	-97.72(12)
O1	Fe1	Si1	Si2	-78.42(6)	O1	Fe1	Si1	Si3	42.01(5)
O1	Fe1	Si1	Si4	161.54(5)	Si1	Fe1	O1[1]	C10[1]	-154.78(13)
Si1	Fe1	O1[1]	C13[1]	50.26(14)	O1[1]	Fe1	Si1	Si2	14.29(7)
O1[1]	Fe1	Si1	Si3	134.73(6)	O1[1]	Fe1	Si1	Si4	-105.75(6)
Si1[1]	Fe1	O1	C10	-154.78(13)	Si1[1]	Fe1	O1	C13	50.26(14)
O1	Fe1	Si1[1]	Si2[1]	14.29(7)	O1	Fe1	Si1[1]	Si3[1]	134.73(6)
O1	Fe1	Si1[1]	Si4[1]	-105.75(6)	Si1[1]	Fe1	O1[1]	C10[1]	57.25(15)
Si1[1]	Fe1	O1[1]	C13[1]	-97.72(12)	O1[1]	Fe1	Si1[1]	Si2[1]	-78.42(6)
O1[1]	Fe1	Si1[1]	Si3[1]	42.01(5)	O1[1]	Fe1	Si1[1]	Si4[1]	161.54(5)
O1	Fe1	O1[1]	C10[1]	-51.19(15)	O1	Fe1	O1[1]	C13[1]	153.84(14)
O1[1]	Fe1	O1	C10	-51.19(15)	O1[1]	Fe1	O1	C13	153.84(14)

Fe1	Si1	Si2	C1	-82.76(4)	Fe1	Si1	Si2	C2	37.72(6)
Fe1	Si1	Si2	C3	157.49(3)	Fe1	Si1	Si3	C4	163.42(3)
Fe1	Si1	Si3	C5	-76.04(4)	Fe1	Si1	Si3	C6	44.31(5)
Fe1	Si1	Si4	C7	41.21(5)	Fe1	Si1	Si4	C8	161.87(4)
Fe1	Si1	Si4	C9	-77.62(6)	Si2	Si1	Si3	C4	-69.60(5)
Si2	Si1	Si3	C5	50.94(4)	Si2	Si1	Si3	C6	171.28(4)
Si3	Si1	Si2	C1	150.92(4)	Si3	Si1	Si2	C2	-88.61(5)
Si3	Si1	Si2	C3	31.17(5)	Si2	Si1	Si4	C7	-85.72(5)
Si2	Si1	Si4	C8	34.94(6)	Si2	Si1	Si4	C9	155.45(4)
Si4	Si1	Si2	C1	44.09(5)	Si4	Si1	Si2	C2	164.57(4)
Si4	Si1	Si2	C3	-75.66(5)	Si3	Si1	Si4	C7	167.00(3)
Si3	Si1	Si4	C8	-72.33(5)	Si3	Si1	Si4	C9	48.18(5)
Si4	Si1	Si3	C4	37.03(5)	Si4	Si1	Si3	C5	157.58(3)
Si4	Si1	Si3	C6	-82.08(4)	Fe1	O1	C10	C11	177.85(13)
Fe1	O1	C13	C12	162.43(14)	C10	O1	C13	C12	3.4(3)
C13	O1	C10	C11	-24.7(3)	C16	O3	C20	C16	0.0(10)
C16	O3	C20	C17	-70.9(14)	C16	O3	C20	C19	-88.6(16)
C20	O3	C16	C17	76.7(14)	C20	O3	C16	C19	55.3(12)
C20	O3	C16	C20	-0.0(10)	C16	O3	C21	C14	15.0(11)
C16	O3	C21	C18	-12.5(10)	C21	O3	C16	C17	-2.5(12)
C21	O3	C16	C19	-23.9(11)	C21	O3	C16	C20	-79.2(12)
C20	O3	C21	C14	-17.1(9)	C20	O3	C21	C18	-44.6(9)
C21	O3	C20	C16	114.7(10)	C21	O3	C20	C17	43.8(9)
C21	O3	C20	C19	26.1(11)	O1	C10	C11	C12	35.4(3)
C10	C11	C12	C13	-32.9(4)	C11	C12	C13	O1	18.5(4)
C17	C14	C18	C17	-0.0(5)	C17	C14	C18	C19	-5.2(8)
C17	C14	C18	C21	-110.5(7)	C18	C14	C17	C16	93.3(16)
C18	C14	C17	C18	0.0(11)	C18	C14	C17	C19	166(2)
C18	C14	C17	C20	123.2(16)	C17	C14	C19	C16	79.7(19)
C17	C14	C19	C17	0.0(12)	C17	C14	C19	C18	13(2)
C17	C14	C19	C20	111(2)	C19	C14	C17	C16	-73(2)
C19	C14	C17	C18	-166(2)	C19	C14	C17	C19	0.0(17)
C19	C14	C17	C20	-43.0(19)	C17	C14	C21	O3	-20.4(11)
C17	C14	C21	C18	68.9(11)	C21	C14	C17	C16	18.7(11)
C21	C14	C17	C18	-74.6(12)	C21	C14	C17	C19	91.7(14)
C21	C14	C17	C20	48.7(10)	C18	C14	C19	C16	66.6(19)
C18	C14	C19	C17	-13(2)	C18	C14	C19	C18	0.0(11)
C18	C14	C19	C20	98.0(19)	C19	C14	C18	C17	5.2(9)
C19	C14	C18	C19	0.0(7)	C19	C14	C18	C21	-105.3(10)

C18	C14	C21	O3	-89.3(13)	C18	C14	C21	C18	0.0(9)
C21	C14	C18	C17	110.5(6)	C21	C14	C18	C19	105.3(8)
C21	C14	C18	C21	0.0(3)	C19	C14	C21	O3	3.0(11)
C19	C14	C21	C18	92.3(13)	C21	C14	C19	C16	-15.2(13)
C21	C14	C19	C17	-94.9(18)	C21	C14	C19	C18	-81.7(14)
C21	C14	C19	C20	16.3(15)	O3	C16	C17	C14	-10.3(11)
O3	C16	C17	C18	16.6(11)	O3	C16	C17	C19	-84.0(14)
O3	C16	C17	C20	-95.3(12)	O3	C16	C19	C14	22.5(12)
O3	C16	C19	C17	100.6(17)	O3	C16	C19	C18	44.1(10)
O3	C16	C19	C20	-92.9(13)	O3	C16	C20	O3	0.0(3)
O3	C16	C20	C17	102.0(8)	O3	C16	C20	C19	97.0(11)
C17	C16	C19	C14	-78.1(19)	C17	C16	C19	C17	-0.0(12)
C17	C16	C19	C18	-56.5(17)	C17	C16	C19	C20	166(2)
C19	C16	C17	C14	74(2)	C19	C16	C17	C18	101(2)
C19	C16	C17	C19	-0.0(16)	C19	C16	C17	C20	-11(2)
C17	C16	C20	O3	-102.0(9)	C17	C16	C20	C17	-0.0(4)
C17	C16	C20	C19	-5.0(7)	C20	C16	C17	C14	85.0(15)
C20	C16	C17	C18	111.9(15)	C20	C16	C17	C19	11.4(17)
C20	C16	C17	C20	-0.0(11)	C19	C16	C20	O3	-97.0(13)
C19	C16	C20	C17	5.0(10)	C19	C16	C20	C19	0.0(7)
C20	C16	C19	C14	115.4(19)	C20	C16	C19	C17	-166(3)
C20	C16	C19	C18	137.0(18)	C20	C16	C19	C20	-0.0(13)
C14	C17	C18	C14	0.0(12)	C14	C17	C18	C21	68.6(16)
C14	C17	C19	C14	0.0(6)	C14	C17	C19	C16	-105.3(9)
C14	C17	C19	C18	-6.2(11)	C14	C17	C19	C20	-112.9(19)
C14	C17	C20	O3	-50.5(10)	C14	C17	C20	C16	-100.0(12)
C16	C17	C18	C14	-92.2(12)	C16	C17	C18	C21	-23.6(11)
C16	C17	C19	C14	105.3(9)	C16	C17	C19	C16	0.0(5)
C16	C17	C19	C18	99.1(10)	C16	C17	C19	C20	-7.7(14)
C16	C17	C20	O3	49.5(13)	C16	C17	C20	C16	-0.0(10)
C18	C17	C19	C14	6.2(10)	C18	C17	C19	C16	-99.1(10)
C18	C17	C19	C18	-0.0(5)	C18	C17	C19	C20	-106.7(16)
C19	C17	C18	C14	-14(2)	C19	C17	C18	C21	55(2)
C18	C17	C20	O3	-27.1(11)	C18	C17	C20	C16	-76.6(13)
C20	C17	C18	C14	-62.6(14)	C20	C17	C18	C21	6.0(13)
C19	C17	C20	O3	-115(3)	C19	C17	C20	C16	-165(3)
C20	C17	C19	C14	113(2)	C20	C17	C19	C16	7.7(15)
C20	C17	C19	C18	106.7(17)	C20	C17	C19	C20	0.0(8)
C14	C18	C19	C14	0.0(14)	C14	C18	C19	C16	-116.7(19)

C14	C18	C19	C17	165(3)	C14	C18	C19	C20	-93(2)
C14	C18	C21	O3	97.3(13)	C14	C18	C21	C14	0.0(10)
C17	C18	C21	O3	22.7(10)	C17	C18	C21	C14	-74.5(11)
C19	C18	C21	O3	38.8(8)	C19	C18	C21	C14	-58.4(9)
C21	C18	C19	C14	67.4(11)	C21	C18	C19	C16	-49.3(9)
C21	C18	C19	C17	-128.1(17)	C21	C18	C19	C20	-26.0(13)
C14	C19	C20	O3	-24.0(15)	C14	C19	C20	C16	-75.2(17)
C16	C19	C20	O3	51.1(13)	C16	C19	C20	C16	-0.0(10)
C17	C19	C20	O3	66(3)	C17	C19	C20	C16	15(3)
C18	C19	C20	O3	2.1(15)	C18	C19	C20	C16	-49.1(17)

Symmetry Operators:

(1) -X+1,Y,-Z+1/2

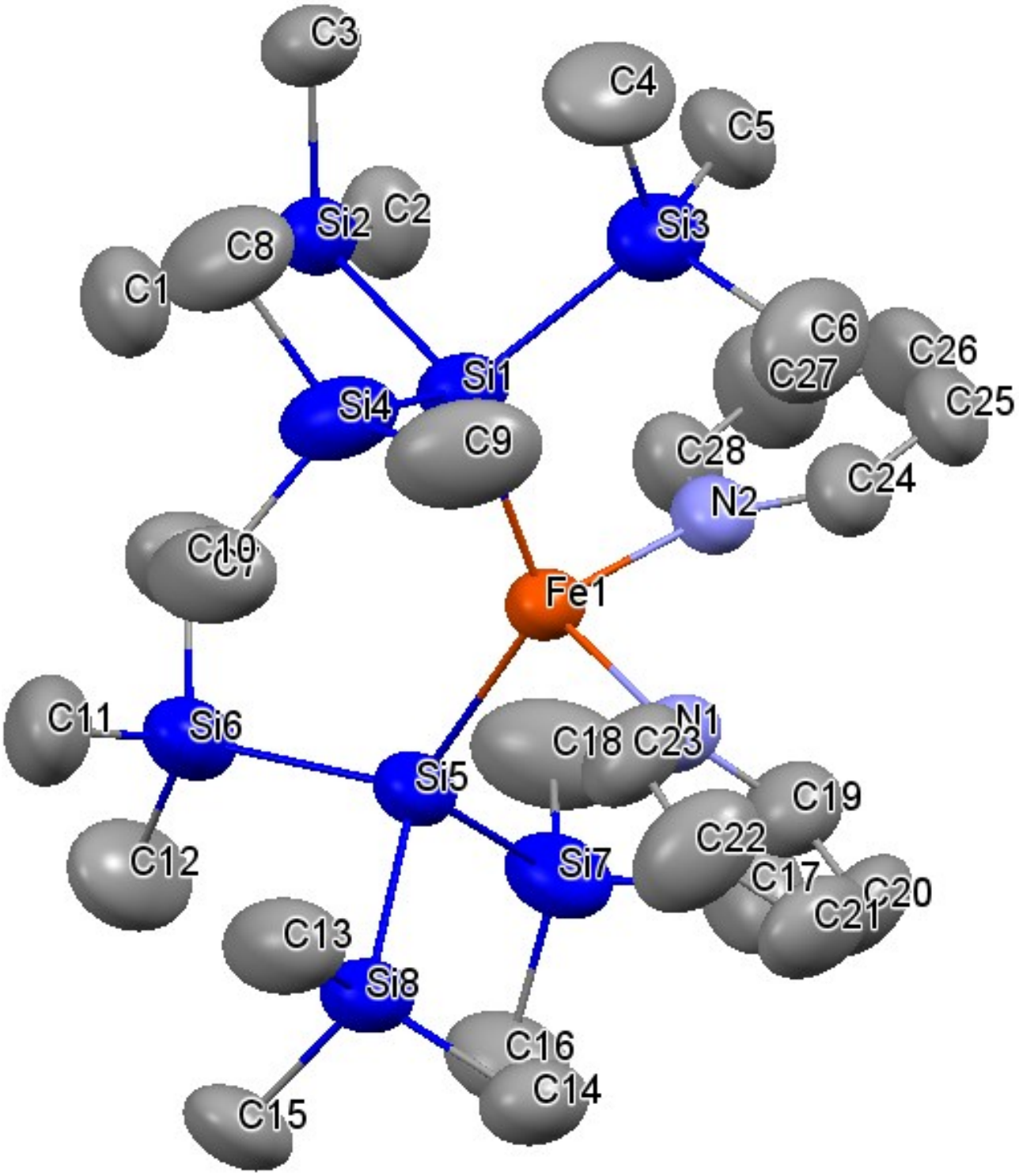

Figure S14. ORTEP drawing of **2** (50% probability of the thermal ellipsoids)

Table S2-1. Crystal data and structure refinement for **2**.

Empirical Formula	$C_{28}H_{64}FeN_2Si_8$
Formula Weight	709.36
Crystal Color, Habit	darkbrown, block
Crystal Dimensions	0.200 X 0.200 X 0.200 mm
Crystal System	triclinic
Lattice Type	Primitive
Lattice Parameters	a = 10.760(3) Å
	b = 12.605(2) Å
	c = 18.063(4) Å
	α = 73.466(10) ^{o}
	β = 81.042(11) ^{o}
	γ = 70.518(9) ^{o}
	V = 2209.0(9) Å^3
Space Group	P-1 (#2)
Z value	2
D_{calc}	1.066 g/cm^3
F_{000}	768.00
μ(MoKα)	5.763 cm^{-1}
Diffractometer	Saturn724
Radiation	MoKα (λ = 0.71075 Å)
	multi-layer mirror monochromated
Voltage, Current	50kV, 24mA
Temperature	-79.8^{o}C
Detector Aperture	72.8 x 72.8 mm
Data Images	720 exposures
ω oscillation Range (χ=45.0, ϕ=0.0)	-70.0 - 110.0^o
Exposure Rate	10.0 sec./^{o}
Detector Swing Angle	19.98^o
ω oscillation Range (χ=45.0, ϕ=90.0)	-70.0 - 110.0^o
Exposure Rate	10.0 sec./^{o}
Detector Swing Angle	19.98^o
Detector Position	44.75 mm
Pixel Size	0.141 mm
$2\theta_{max}$	55.0^o
No. of Reflections Measured	Total: 18470
	Unique: 9756 (R_{int} = 0.0382)
Corrections	Lorentz-polarization

	Absorption (trans. factors: 0.778 - 0.891)
Structure Solution	Direct Methods (SIR2008)
Refinement	Full-matrix least-squares on F^2
Function Minimized	Σ w $(Fo^2 - Fc^2)^2$
Least Squares Weights	$w = 1/ [\sigma^2(Fo^2) + (0.0424 \cdot P)^2 + 0.3108 \cdot P]$ where $P = (Max(Fo^2,0) + 2Fc^2)/3$
$2\theta_{max}$ cutoff	55.0^o
Anomalous Dispersion	All non-hydrogen atoms
No. Observations (All reflections)	9756
No. Variables	352
Reflection/Parameter Ratio	27.72
Residuals: R1 (I>2.00σ(I))	0.0495
Residuals: R (All reflections)	0.0856
Residuals: wR2 (All reflections)	0.1100
Goodness of Fit Indicator	1.040
Max Shift/Error in Final Cycle	0.000
Maximum peak in Final Diff. Map	0.35 $e^-/Å^3$
Minimum peak in Final Diff. Map	-0.27 $e^-/Å^3$

Table S2-2. Atomic coordinates and B_{iso}/B_{eq} and occupancy

atom	x	y	z	B_{eq}	occ
Fe1	0.11671(4)	0.29098(3)	0.26500(2)	2.367(9)	
Si1	-0.11543(7)	0.42150(6)	0.28608(4)	2.496(13)	
Si2	-0.23210(7)	0.48690(6)	0.17440(4)	2.574(14)	
Si3	-0.11542(9)	0.59710(7)	0.30757(5)	3.548(17)	
Si4	-0.26267(8)	0.35748(7)	0.38526(5)	3.630(17)	
Si5	0.21126(7)	0.11299(6)	0.21017(4)	2.539(14)	
Si6	0.09494(9)	0.07596(7)	0.12502(5)	3.659(18)	
Si7	0.42456(8)	0.09755(7)	0.14867(5)	3.367(17)	
Si8	0.24432(8)	-0.05625(6)	0.31183(5)	2.781(14)	
N1	0.2090(2)	0.23889(18)	0.37219(13)	2.65(4)	
N2	0.2172(2)	0.41325(18)	0.20260(13)	2.70(4)	
C1	-0.3029(3)	0.3754(3)	0.16304(19)	4.17(7)	
C2	-0.1209(3)	0.5205(3)	0.08664(16)	3.70(6)	
C3	-0.3727(3)	0.6248(2)	0.17051(18)	3.66(6)	
C4	-0.2817(4)	0.6862(3)	0.3417(2)	5.52(9)	
C5	-0.0626(3)	0.6944(3)	0.2176(2)	4.58(7)	
C6	-0.0015(4)	0.5707(3)	0.3850(2)	5.48(9)	
C7	-0.2416(3)	0.2005(3)	0.3953(2)	5.13(8)	
C8	-0.4429(3)	0.4377(3)	0.3702(2)	5.01(8)	
C9	-0.2349(4)	0.3719(3)	0.48190(18)	5.47(8)	
C10	0.0340(4)	0.2058(3)	0.0430(2)	5.65(9)	
C11	-0.0525(3)	0.0345(3)	0.1781(2)	5.51(9)	
C12	0.1957(4)	-0.0435(3)	0.0771(2)	5.68(9)	
C13	0.0931(3)	-0.0479(3)	0.38038(19)	4.51(7)	
C14	0.3846(3)	-0.0796(3)	0.37073(17)	3.72(6)	
C15	0.2803(3)	-0.1954(2)	0.28144(18)	4.02(6)	
C16	0.5269(3)	-0.0544(3)	0.1462(2)	4.47(7)	
C17	0.5235(3)	0.1503(3)	0.1984(2)	5.34(9)	
C18	0.4191(4)	0.1861(3)	0.04529(19)	5.91(9)	
C19	0.3366(3)	0.2212(3)	0.37865(19)	3.66(6)	
C20	0.3963(3)	0.1729(3)	0.4480(2)	4.27(7)	
C21	0.3226(3)	0.1403(3)	0.51339(19)	4.35(7)	
C22	0.1919(3)	0.1571(3)	0.50831(19)	4.93(8)	
C23	0.1391(3)	0.2071(3)	0.43764(18)	3.85(6)	
C24	0.2632(3)	0.4758(2)	0.23414(18)	3.38(6)	
C25	0.3115(3)	0.5641(3)	0.1912(2)	4.28(7)	
C26	0.3135(3)	0.5910(3)	0.1128(2)	4.84(7)	

C27	0.2668(4)	0.5282(3)	0.0790(2)	5.02(8)
C28	0.2213(3)	0.4401(3)	0.12568(17)	3.54(6)

$B_{eq} = 8/3\ \pi^2(U_{11}(aa^*)^2 + U_{22}(bb^*)^2 + U_{33}(cc^*)^2 + 2U_{12}(aa^*bb^*)\cos\gamma + 2U_{13}(aa^*cc^*)\cos\beta + 2U_{23}(bb^*cc^*)\cos\alpha)$

Table S2-3. Anisotropic displacement parameters

atom	U_{11}	U_{22}	U_{33}	U_{12}	U_{13}	U_{23}
Fe1	0.0293(2)	0.02586(19)	0.0338(2)	-0.00441(15)	-0.00615(16)	-0.00853(17)
Si1	0.0295(4)	0.0290(4)	0.0301(4)	-0.0030(3)	-0.0029(3)	-0.0046(3)
Si2	0.0342(4)	0.0296(4)	0.0334(4)	-0.0094(3)	-0.0063(3)	-0.0051(3)
Si3	0.0483(5)	0.0392(5)	0.0481(5)	-0.0021(4)	-0.0129(4)	-0.0205(4)
Si4	0.0329(5)	0.0470(5)	0.0404(5)	-0.0024(4)	0.0022(4)	0.0021(4)
Si5	0.0350(4)	0.0249(4)	0.0359(4)	-0.0070(3)	-0.0044(3)	-0.0081(3)
Si6	0.0585(6)	0.0298(4)	0.0528(6)	-0.0081(4)	-0.0212(4)	-0.0108(4)
Si7	0.0436(5)	0.0314(4)	0.0468(5)	-0.0071(4)	0.0084(4)	-0.0117(4)
Si8	0.0355(4)	0.0272(4)	0.0375(4)	-0.0046(3)	-0.0034(4)	-0.0052(3)
N1	0.0320(12)	0.0337(12)	0.0333(13)	-0.0043(10)	-0.0066(10)	-0.0103(10)
N2	0.0302(12)	0.0294(12)	0.0422(14)	-0.0067(10)	-0.0019(10)	-0.0110(11)
C1	0.053(2)	0.0517(19)	0.062(2)	-0.0261(16)	-0.0056(17)	-0.0140(17)
C2	0.056(2)	0.0558(19)	0.0357(17)	-0.0271(16)	-0.0032(15)	-0.0107(15)
C3	0.0406(17)	0.0384(16)	0.054(2)	-0.0053(14)	-0.0143(15)	-0.0044(15)
C4	0.072(3)	0.058(2)	0.076(3)	0.0080(19)	-0.014(2)	-0.041(2)
C5	0.068(2)	0.0360(17)	0.077(3)	-0.0213(16)	-0.0166(19)	-0.0109(17)
C6	0.073(3)	0.081(3)	0.060(2)	-0.012(2)	-0.017(2)	-0.036(2)
C7	0.044(2)	0.051(2)	0.078(3)	-0.0122(16)	0.0063(18)	0.0082(19)
C8	0.0362(18)	0.074(2)	0.058(2)	-0.0059(17)	0.0049(16)	-0.0003(19)
C9	0.070(3)	0.076(2)	0.0353(19)	-0.003(2)	0.0038(17)	0.0011(18)
C10	0.102(3)	0.048(2)	0.063(2)	-0.013(2)	-0.038(2)	-0.0063(18)
C11	0.059(2)	0.057(2)	0.104(3)	-0.0214(18)	-0.031(2)	-0.019(2)
C12	0.099(3)	0.054(2)	0.070(3)	-0.008(2)	-0.027(2)	-0.033(2)
C13	0.047(2)	0.0477(19)	0.061(2)	-0.0105(16)	0.0051(17)	-0.0004(17)
C14	0.0470(19)	0.0420(17)	0.0448(18)	-0.0037(14)	-0.0098(15)	-0.0075(14)
C15	0.066(2)	0.0270(15)	0.056(2)	-0.0103(14)	-0.0084(17)	-0.0077(14)
C16	0.054(2)	0.0407(18)	0.065(2)	-0.0051(15)	0.0108(17)	-0.0175(17)
C17	0.042(2)	0.069(2)	0.100(3)	-0.0235(18)	0.015(2)	-0.037(2)
C18	0.084(3)	0.060(2)	0.053(2)	-0.008(2)	0.022(2)	-0.0027(19)
C19	0.0360(17)	0.0488(18)	0.051(2)	-0.0085(14)	-0.0028(14)	-0.0122(16)

C20	0.0364(18)	0.064(2)	0.063(2)	-0.0068(16)	-0.0210(17)	-0.0177(19)
C21	0.055(2)	0.065(2)	0.045(2)	-0.0028(17)	-0.0221(17)	-0.0204(18)
C22	0.050(2)	0.092(3)	0.0366(19)	-0.015(2)	-0.0015(16)	-0.0112(19)
C23	0.0324(16)	0.065(2)	0.0458(19)	-0.0084(15)	-0.0063(14)	-0.0139(17)
C24	0.0421(17)	0.0389(16)	0.0522(19)	-0.0106(14)	-0.0081(14)	-0.0186(15)
C25	0.053(2)	0.0391(17)	0.080(3)	-0.0184(15)	-0.0138(18)	-0.0197(18)
C26	0.065(2)	0.047(2)	0.075(3)	-0.0328(18)	-0.011(2)	0.0031(19)
C27	0.083(3)	0.066(2)	0.047(2)	-0.039(2)	-0.0040(19)	-0.0013(18)
C28	0.055(2)	0.0442(17)	0.0414(18)	-0.0218(15)	-0.0076(15)	-0.0092(14)

The general temperature factor expression: $\exp(-2\pi^2(a^{*2}U_{11}h^2 + b^{*2}U_{22}k^2 + c^{*2}U_{33}l^2 + 2a^*b^*U_{12}hk + 2a^*c^*U_{13}hl + 2b^*c^*U_{23}kl))$

Table S2-4. Bond lengths (Å)

atom	atom	distance	atom	atom	distance
Fe1	Si1	2.5317(9)	Fe1	Si5	2.5451(10)
Fe1	N1	2.146(2)	Fe1	N2	2.135(2)
Si1	Si2	2.3402(12)	Si1	Si3	2.3535(14)
Si1	Si4	2.3487(12)	Si2	C1	1.877(4)
Si2	C2	1.868(3)	Si2	C3	1.877(3)
Si3	C4	1.885(3)	Si3	C5	1.874(3)
Si3	C6	1.889(4)	Si4	C7	1.873(4)
Si4	C8	1.886(3)	Si4	C9	1.883(4)
Si5	Si6	2.3553(15)	Si5	Si7	2.3601(12)
Si5	Si8	2.3488(10)	Si6	C10	1.873(3)
Si6	C11	1.872(4)	Si6	C12	1.885(4)
Si7	C16	1.873(3)	Si7	C17	1.868(5)
Si7	C18	1.881(3)	Si8	C13	1.877(3)
Si8	C14	1.877(4)	Si8	C15	1.886(3)
N1	C19	1.333(4)	N1	C23	1.334(4)
N2	C24	1.340(5)	N2	C28	1.330(4)
C19	C20	1.382(5)	C20	C21	1.357(5)
C21	C22	1.364(5)	C22	C23	1.371(5)
C24	C25	1.371(5)	C25	C26	1.358(6)
C26	C27	1.375(7)	C27	C28	1.373(5)

Table S2-5. Bond angles (°)

atom	atom	atom	angle	atom	atom	atom	angle
Si1	Fe1	Si5	133.60(4)	Si1	Fe1	N1	107.02(6)
Si1	Fe1	N2	102.21(6)	Si5	Fe1	N1	103.74(6)
Si5	Fe1	N2	106.99(7)	N1	Fe1	N2	97.97(10)
Fe1	Si1	Si2	111.83(4)	Fe1	Si1	Si3	111.83(4)
Fe1	Si1	Si4	121.14(3)	Si2	Si1	Si3	101.95(4)
Si2	Si1	Si4	104.29(5)	Si3	Si1	Si4	103.78(4)
Si1	Si2	C1	111.76(10)	Si1	Si2	C2	110.28(11)
Si1	Si2	C3	114.25(12)	C1	Si2	C2	108.11(16)
C1	Si2	C3	106.93(15)	C2	Si2	C3	105.14(13)
Si1	Si3	C4	114.04(15)	Si1	Si3	C5	111.94(13)
Si1	Si3	C6	111.51(13)	C4	Si3	C5	105.73(14)
C4	Si3	C6	105.16(18)	C5	Si3	C6	107.99(18)
Si1	Si4	C7	110.13(11)	Si1	Si4	C8	114.83(11)
Si1	Si4	C9	112.27(14)	C7	Si4	C8	106.33(17)
C7	Si4	C9	107.53(17)	C8	Si4	C9	105.31(16)
Fe1	Si5	Si6	121.57(4)	Fe1	Si5	Si7	112.75(4)
Fe1	Si5	Si8	109.59(4)	Si6	Si5	Si7	105.11(5)
Si6	Si5	Si8	102.44(5)	Si7	Si5	Si8	103.53(4)
Si5	Si6	C10	112.36(15)	Si5	Si6	C11	110.07(15)
Si5	Si6	C12	114.21(14)	C10	Si6	C11	107.47(17)
C10	Si6	C12	104.84(16)	C11	Si6	C12	107.51(19)
Si5	Si7	C16	114.19(12)	Si5	Si7	C17	111.75(12)
Si5	Si7	C18	112.14(12)	C16	Si7	C17	105.37(16)
C16	Si7	C18	106.29(16)	C17	Si7	C18	106.52(19)
Si5	Si8	C13	110.55(9)	Si5	Si8	C14	112.70(10)
Si5	Si8	C15	115.18(10)	C13	Si8	C14	106.60(15)
C13	Si8	C15	105.55(16)	C14	Si8	C15	105.64(14)
Fe1	N1	C19	125.16(19)	Fe1	N1	C23	118.2(2)
C19	N1	C23	116.1(3)	Fe1	N2	C24	125.31(19)
Fe1	N2	C28	117.7(2)	C24	N2	C28	116.5(3)
N1	C19	C20	123.5(3)	C19	C20	C21	118.9(3)
C20	C21	C22	118.8(3)	C21	C22	C23	119.1(3)
N1	C23	C22	123.7(3)	N2	C24	C25	123.2(3)
C24	C25	C26	119.4(4)	C25	C26	C27	118.5(3)
C26	C27	C28	118.8(3)	N2	C28	C27	123.5(4)

Table S2-6. Torsion Angles(O)

(Those having bond angles > 160 or < 20 degrees are excluded.)

atom1	atom2	atom3	atom4	angle	atom1	atom2	atom3	atom4	angle
Si1	Fe1	Si5	Si6	23.26(5)	Si1	Fe1	Si5	Si7	149.37(3)
Si1	Fe1	Si5	Si8	-95.89(4)	Si5	Fe1	Si1	Si2	-50.50(5)
Si5	Fe1	Si1	Si3	-164.13(3)	Si5	Fe1	Si1	Si4	73.06(5)
Si1	Fe1	N1	C19	-145.56(15)	Si1	Fe1	N1	C23	43.54(16)
N1	Fe1	Si1	Si2	-179.88(7)	N1	Fe1	Si1	Si3	66.49(8)
N1	Fe1	Si1	Si4	-56.32(8)	Si1	Fe1	N2	C24	80.04(14)
Si1	Fe1	N2	C28	-91.58(12)	N2	Fe1	Si1	Si2	77.73(8)
N2	Fe1	Si1	Si3	-35.90(8)	N2	Fe1	Si1	Si4	-158.71(8)
Si5	Fe1	N1	C19	69.62(18)	Si5	Fe1	N1	C23	-101.27(14)
N1	Fe1	Si5	Si6	153.72(7)	N1	Fe1	Si5	Si7	-80.17(7)
N1	Fe1	Si5	Si8	34.57(8)	Si5	Fe1	N2	C24	-136.46(12)
Si5	Fe1	N2	C28	51.92(13)	N2	Fe1	Si5	Si6	-103.34(7)
N2	Fe1	Si5	Si7	22.77(7)	N2	Fe1	Si5	Si8	137.51(7)
N1	Fe1	N2	C24	-29.39(15)	N1	Fe1	N2	C28	158.99(12)
N2	Fe1	N1	C19	-40.13(18)	N2	Fe1	N1	C23	148.98(15)
Fe1	Si1	Si2	C1	81.52(5)	Fe1	Si1	Si2	C2	-38.76(5)
Fe1	Si1	Si2	C3	-156.90(4)	Fe1	Si1	Si3	C4	-169.34(3)
Fe1	Si1	Si3	C5	70.68(5)	Fe1	Si1	Si3	C6	-50.43(5)
Fe1	Si1	Si4	C7	-37.81(7)	Fe1	Si1	Si4	C8	-157.78(4)
Fe1	Si1	Si4	C9	81.96(6)	Si2	Si1	Si3	C4	71.04(5)
Si2	Si1	Si3	C5	-48.94(5)	Si2	Si1	Si3	C6	-170.05(4)
Si3	Si1	Si2	C1	-158.86(4)	Si3	Si1	Si2	C2	80.86(5)
Si3	Si1	Si2	C3	-37.28(5)	Si2	Si1	Si4	C7	89.22(5)
Si2	Si1	Si4	C8	-30.75(6)	Si2	Si1	Si4	C9	-151.00(4)
Si4	Si1	Si2	C1	-51.09(5)	Si4	Si1	Si2	C2	-171.37(4)
Si4	Si1	Si2	C3	70.49(5)	Si3	Si1	Si4	C7	-164.37(4)
Si3	Si1	Si4	C8	75.67(6)	Si3	Si1	Si4	C9	-44.59(5)
Si4	Si1	Si3	C4	-37.13(5)	Si4	Si1	Si3	C5	-157.11(4)
Si4	Si1	Si3	C6	81.79(5)	Fe1	Si5	Si6	C10	49.77(6)
Fe1	Si5	Si6	C11	-69.96(5)	Fe1	Si5	Si6	C12	169.01(3)
Fe1	Si5	Si7	C16	154.60(4)	Fe1	Si5	Si7	C17	35.12(5)
Fe1	Si5	Si7	C18	-84.42(6)	Fe1	Si5	Si8	C13	48.38(6)
Fe1	Si5	Si8	C14	-70.81(5)	Fe1	Si5	Si8	C15	167.89(4)
Si6	Si5	Si7	C16	-70.88(5)	Si6	Si5	Si7	C17	169.64(4)
Si6	Si5	Si7	C18	50.11(6)	Si7	Si5	Si6	C10	-79.73(5)
Si7	Si5	Si6	C11	160.54(4)	Si7	Si5	Si6	C12	39.52(5)

Si6	Si5	Si8	C13	-81.98(6)	Si6	Si5	Si8	C14	158.84(4)
Si6	Si5	Si8	C15	37.53(5)	Si8	Si5	Si6	C10	172.35(4)
Si8	Si5	Si6	C11	52.62(5)	Si8	Si5	Si6	C12	-68.41(5)
Si7	Si5	Si8	C13	168.89(5)	Si7	Si5	Si8	C14	49.71(6)
Si7	Si5	Si8	C15	-71.60(6)	Si8	Si5	Si7	C16	36.25(7)
Si8	Si5	Si7	C17	-83.23(5)	Si8	Si5	Si7	C18	157.24(5)
Fe1	N1	C19	C20	-171.01(19)	Fe1	N1	C23	C22	170.6(2)
C19	N1	C23	C22	-1.1(5)	C23	N1	C19	C20	0.1(4)
Fe1	N2	C24	C25	-171.13(14)	Fe1	N2	C28	C27	170.98(16)
C24	N2	C28	C27	-1.4(3)	C28	N2	C24	C25	0.6(3)
N1	C19	C20	C21	0.7(5)	C19	C20	C21	C22	-0.4(5)
C20	C21	C22	C23	-0.6(6)	C21	C22	C23	N1	1.4(6)
N2	C24	C25	C26	0.1(4)	C24	C25	C26	C27	-0.0(4)
C25	C26	C27	C28	-0.7(4)	C26	C27	C28	N2	1.5(4)

Reference

(1) (a) C. Marschner, *Eur. J. Inorg. Chem.* 1998, 221-226; (b) C. Kayser, R. Fischer, J. Baumgartner, C. Marschner, *Organometallics* 2002, **21**, 1023-1030.

(2) (a) M. Yuki, H. Tanaka, K. Sasaki, Y. Miyake, K. Yoshizawa and Y. Nishibayashi, *Nat. Commun*. 2012, **3**, 1-6/2264. (b) R. Araake, K. Sakadani, M. Tada, Y. Sakai, Y. Ohki, *J. Am. Chem. Soc*. 2017, **139**, 5596-5606. (c) D. E. Prokopchuk, E. S. Wiedner, E. D. Walter, C. V. Popescu, N. A. Piro, W. S. Kassel, R. Morris Bullock, M. T. Mock, *J. Am. Chem. Soc*. 2017, **139**, 9291-9301.

(3) SIR2008: M. C. Burla, R. Caliandro, M. Camalli, B. Carrozzini, G. L. Cascarano, L. De Caro, C. Giacovazzo, G. Polidori, D. Siliqi, R. Spagna, *J. Appl. Cryst.* 2007, **40**, 609-613.

(4) International Tables for Crystallography, Vol.C (1992). Ed. A. J. C. Wilson, Kluwer Academic Publishers, Dordrecht, Netherlands, Table 6.1.1.4, pp. 572.

(5) J. A. Ibers, W. C. Hamilton, *Acta Cryst*. 1964, **17**, 781-782.

(6) D. C. Creagh and W. J. McAuley, in International Tables for Crystallography, Vol C; Ed. A. J. C. Wilson, Kluwer Academic Publishers, Dordrecht, Netherlands, Table 4.2.6.8, pages 219-222, 1992.

(7) D. C. Creagh, and J. H. Hubbell, in International Tables for Crystallography, Vol C; Ed. A. J. C. Wilson, Kluwer Academic Publishers, Boston, Table 4.2.4.3, pages 200-206, 1992.

(8) CrystalStructure 4.2.5: Crystal Structure Analysis Package, Rigaku Corporation (2000-2017). Tokyo 196-8666, Japan.

(9) SHELXL Version 2017/1: G. M. Sheldrick, *Acta Cryst*. 2008, **A64**, 112-122.